

Modelling of the dynamic system and designing a gentle and robust control system for the knee joint of the gait rehabilitation robot LOPES.

Henk van Twillert

Supervisors

prof.dr.ir. J. van Amerongen
dr.ir. S. Stramigioli
dr.ir. H. van der Kooy, drs.ir. J.F.Veneman, ir. R. Ekkelenkamp

March 2005

Report nr. 011CE2005
Control Engineering
EE-Math-CS
University of Twente
P.O. Box 217
7500 AE Enschede
The Netherlands

Summary

This project is a part of the LOPES (LOpes extremity Powered ExoSkeleton) project at the University of Twente. This exoskeleton will be designed to get a rehabilitation robot for stroke patients. The robot should be able to assist the therapists, who currently perform the rehabilitation treatment. The assignment discussed in this report deals with the knee joint of the exoskeleton.

The goal of this assignment consists of two parts: first has the dynamic system of the knee been modelled and the second part is to design a gentle and robust controller for the dynamic system.

The modelling of the dynamic system of the knee joint is discussed in chapter two. First is the knee joint converted in an Ideal Physical Model (IPM) to get an orderly description of the system. This IPM is converted in a 4th order mechanical model consisted of two domains; the motor rotation domain and the cable translation domain. This 4th order model is used to develop a block scheme. The different parameters used in the models are determined, estimated or were known from datasheets.

The open loop transfer of the dynamic system of the knee joint and the open loop transfer of the model are compared. The magnitudes of the frictions are changed to find the best match of the model with the real system.

The 4th order model gives some numerical problems due to huge value differences in the A matrix. To solve this problem, the 4th order model is converted in a 2nd order one. This 2nd order system is used to design the controller.

Chapter three deals with the controller design to control the knee joint. The chosen method to control this dynamic system is the Linear Quadratic Gaussian (LQG) controller. The LQG algorithm provides an optimal feedback for systems with deterministic parameters and takes in account the process disturbances and measurement noise. The LQG consist of a Linear Quadratic Regulator to get an optimal feedback and a Linear Quadratic Estimator to estimate the states of the system based on the model. The motor current will be controlled and the measurement spring length is the output of the system. The necessary matrices (Q and R for LQR and Q, R and G for LQE) are determined and give a system with acceptable errors together with realistic torque commands. A parameter variation is done, based on the simulations. A friction rise of 220% can be reached, but this is a theoretical value, because the force commands become to unrealistic high levels.

The test results are discussed in chapter 4. The measurement spring of the exoskeleton is changed. An open loop transfer of the dynamic system is measured and the model is re-tuned to get the best match. The bodeplots concerning closed loop transfer of both simulation and measurement are compared - the differences between those two bodeplots are acceptable and the simulation is useful to make predictions of the (controlled) system behaviour

The conclusion of this assignment is that the model can be used for model based control. The LQG controller controls the system acceptable. The test results show a good controller for the knee joint connected with the fixed world.

Samenvatting

Dit project is onderdeel van het LOPES (Lower extremity Powered Exoskeleton) project aan de Universiteit Twente. Het exoskelet wordt ontworpen om uiteindelijk een revalidatie robot te krijgen die mensen met een hersenbloeding helpt revalideren. De robot moet in staat zijn de therapeuten die regelmatig revalidatie behandelingen uitvoeren te assisteren. Deze opdracht behandelt het kniegewricht van de het exoskelet.

Het doel van deze opdracht is bestaat uit twee delen: eerst wordt het dynamische gedrag van het kniegewricht gemodelleerd worden, het tweede deel is het ontwerpen van een robuuste regelaar die het dynamische systeem op een soepele wijze laat functioneren.

Het modelleren van het dynamische systeem is in hoofdstuk 2 behandeld. Eerst is het dynamische systeem omgezet in een Ideaal Fysisch Model (IPM) om zo een ordelijke beschrijving van het systeem te verkrijgen. Dit IPM is omgezet in een 4^e orde mechanisch model en bestaat uit twee domeinen: het motor rotatie domein en het kabel translatie domein. Dit 4^e orde systeem is gebruikt voor het maken van een blokschema. De verschillende parameters die in deze modellen gebruikt zijn bepaald, geschat of waren bekend van datasheets.

De open loop overdracht van het dynamisch systeem van het kniegewricht en het model zijn vergeleken. De grote van de wrijvingen zijn aangepast, zodat het model zo goed mogelijk het gedrag van het dynamische systeem volgt.

Het 4^e orde systeem geeft wat numerieke problemen door de grote verschillen in de waarden binnen de A matrix. Dit probleem is opgelost door het 4^e order model om te zetten in een 2^e order model. Het 2^e model wordt gebruikt voor het ontwerpen van de regelaar.

Hoofdstuk 3 gaat over het regelaars ontwerp. Om het dynamische systeem te regelen is er gekozen voor de Linear Quadratic Gaussian (LQG) regelaar. Het LQG algoritme geeft een optimale terugkoppeling voor systemen met deterministische parameters, terwijl gelijktijdig rekening gehouden wordt met de procesverstoringen en de meetruis. De LQG regelaar bestaat uit een Linear Quadratic Regulator, om een optimale terugkoppeling te krijgen en een Linear Quadratic Estimator, voor het schatten van de systeemtoestanden op basis van het model. De motor stroom wordt gestuurd en de lengte van de meetveer is de uitgang van het systeem. De nodige matrices (Q en R voor de LQR en Q, R en G voor de LQE) zijn bepaald en regelaar regelt het systeem zodat er een acceptabele fout optreedt, samen met realistische stuurcommando's. Verder is er een parameter variatie uitgevoerd, gebaseerd op de simulaties. De wrijving kan oplopen tot 220%, alleen is dit wel theoretisch, want de stuurcommando's krijgen onrealistische waarden.

De test resultaten zijn besproken in hoofdstuk 4. De meetveer van het exoskelet is vervangen. Het open loop gedrag van het dynamische systeem is opnieuw bekeken en het model in opnieuw aangepast, zodat er weer een goede overeenkomst tussen beide is. De bodeplots van de gesloten loop overdracht zijn vergeleken. De verschillen tussen deze twee bodeplots zijn acceptabel klein en de simulatie kan gebruikt worden voor het geven van een schatting van het systeemgedrag.

De conclusie aan het einde van deze opdracht is dat het gemaakte model gebruikt kan worden voor een op een model gebaseerde regelaar. De LQG regelt het systeem op een accepteerbare manier. De testresultaten laten een goede regelaar zien voor het kniegewricht in geblokkeerde toestand.

Voorwoord

De afgelopen 4 maanden heb ik een pre-doctorale opdracht uitgevoerd bij de vakgroep Biomedische Werktuigbouwkunde aan de Universiteit van Twente. Een pre-doctorale opdracht is een onderdeel van de verkorte opleiding voor studenten met een HBO-achtergrond, als voorbereiding op de doctoraalopdracht.

In september 2002 ben ik begonnen met de verkorte opleiding Elektrotechniek aan de Universiteit van Twente. Nu, tweeënhalf jaar later, zal ik per 1 januari te beginnen met de afstudeeropdracht. Juli 2005 hoop ik deze opdracht te voltooien en dan tegelijk mijn studie af te ronden.

De gigantische inzet van Ralf Ekkelenkamp en Jan Veneman ligt mede ten grondslag aan het resultaat van dit verslag. Zonder hun hulp en goede adviezen zou ik niet zo ver gekomen zijn. Verder wil ik nog mijn mede-Lopeslabgenoten Laurens en Jasper bedanken voor de gezellige tijd. Ook ben ik ook veel dank verschuldigd aan mijn vriendin, die dit verslag nauwkeurig gecorrigeerd heeft.

Ik ben ervan overtuigd, dat de kennis en vaardigheden die ik in de afgelopen maanden opgedaan heb, nuttig zullen zijn voor zowel mijn doctoraalopdracht als voor mijn beroepsperspectieven.

Henk van Twillert
Putten, december 2004

Table of contents

- 1. Introduction**..... 6
 - 1.1 Cerebro Vascular Accident..... 6
 - 1.2 LOPES – project..... 6
 - 1.3 The knee..... 7
 - 1.4 Goals and objectives..... 8

- 2. Model**..... 9
 - 2.1 Ideal Physical Model..... 9
 - 2.2 Mechanical model..... 10
 - 2.3 Parameters..... 10
 - 2.4 Measurement versus model..... 15
 - 2.5 Adaptation of the 4th order model..... 17

- 3. Controller**..... 18
 - 3.1 Choice of the controller..... 18
 - 3.2 Optimal LQG Control..... 19
 - 3.3 LQG used in LOPES..... 23
 - 3.4 Parameter variation..... 26

- 4. Test results**..... 30
 - 4.1 Transfer open loop system with new parameter..... 30
 - 4.2 Test results..... 31

- 5. Conclusion and Recommendations**..... 34
 - 5.1 Conclusion..... 34
 - 5.2 Recommendations..... 35

- 6. References**..... 36

- 7. Annexes**
 - A Datasheets
 - B MRAS (Model Reference Adaptive Control)

1. Introduction

This chapter deals with the background of this pre-doctoral project. In order to give some general insight, themes related to this assignment are discussed. In the first paragraph CVA will be discussed, followed by a paragraph about the LOPES rehabilitation robot. The fourth paragraph explains the major part of the Exoskeleton for this assignment. Finally the goal and objectives are stated.

1.1 CerebroVascular Accident

CerebroVascular Accident (CVA) is the proper medical name for a stroke. Strokes occur when blood vessels in the brain become blocked by clotted blood or build-up of plaque on the inner walls of the vessels. The after effects of a stroke can vary from mild hemiparalysis to death. CVA is one of the leading causes of brain damage and death in the world, behind heart diseases and cancer.

Since a stroke affects the brain, the after effects often influence the motor control of the patient. Literature shows that in general the symptoms involve weakened muscles, spasticity and disordered muscle activation [1]. This causes serious impairments to the gait cycle of these patients. The gait of CVA patients is characterised by a reduced range of motion of all the joints. Rehabilitation is important after a stroke. Many basic functions, such as walking, have to be relearned [2]. This is a long and hard process, but necessary to get a better life.

1.2 LOPES – project

A rehabilitation robot is developed to support the therapist in the rehabilitation process. There were some other commercial rehabilitation robots designed, but none of these robots are ‘interactive’. The assignment for a new project sounds: develop an adaptable actuation method that is not solely position controlled but can also be force controlled. This makes selective support of the gait functions possible. This is the start of the LOPES project. LOPES stands for LOWER extremity Powered ExoSkeleton and is being developed at the University of Twente. Aiming points of LOPES are to induce an active role of the patient in the rehabilitation and offering the therapist more tools to treat the patients.

The prototype exoskeleton is shown in figure 1.1 and consists of three parts, the frame, the hip with the moving parts, and the knee. The patient stands in the frame, while the hip and the knee are connected with the leg. The intention is to keep the frame light by using mass compensation and by placing the motors out from the moving parts of the frame. The hip and knee are driven and controlled individually. The control of the knee will be the assignment for this project.



Figure 1.1: The exoskeleton, consisting of the frame, the hip and the knee

1.3 The knee

This part of the LOPES project deals with the knee. A schematic representation of the knee and actuator is given in figure 1.2. The knee will be driven by an AC synchronous servomotor. The motor is connected to disc 1 through a gear box. This disc converts the rotational movement into a translational movement. Two Bowden cables are fixed on the disc. The Bowden cables are connected with disc 2, into the mechanical knee. The Bowden cables are connected with disc 2, into the mechanical knee.

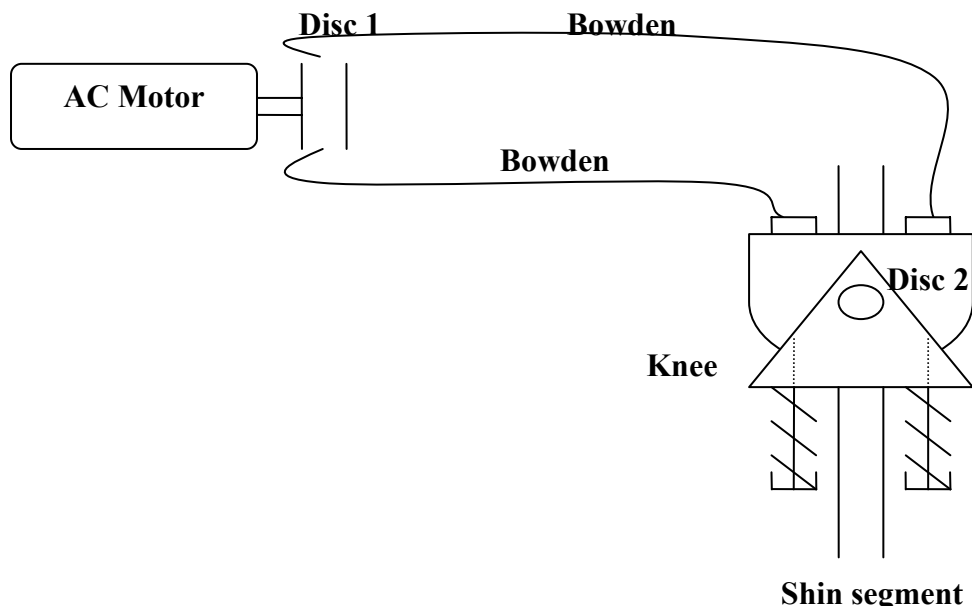


Figure 1.2 Schematic representation of the knee and actuator.

The knee has been developed in earlier states of the LOPES project [3]. Figure 1.3 shows a drawing of the knee. The knee consists of two moveable discs. One disc is connected to two transmission cables (Bowden cables). The other disc is connected (also with Bowden cables) to the shinbone of the exoskeleton.

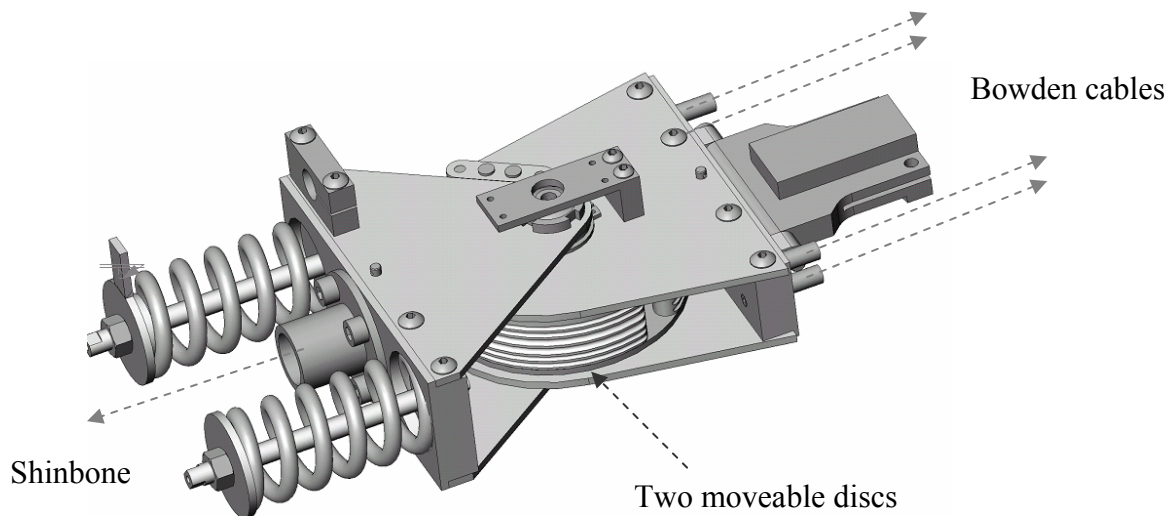


Figure 1.3: The knee.

As mentioned, the knee will be driven by a synchronic motor. The system contains a lot of friction, particularly in the cables. The problem is how to control this system.

1.4 Goal and objectives

The problem mentioned at the end of the previous paragraph leads to a goal for this pre-doctoral assignment. The problem can be divided in two parts:

- **Model the system** and the dynamic behaviour into a working simulation in order to design the controller.
- **Design a gentle and robust control system** for the knee of the exoskeleton.
 - **Gentle:** The aim of the exoskeleton is helping people to rehabilitate. Due to the combination of people and robots, the robot must be gentle. The word ‘gentle’ here means that movements have to be balanced, by phases and without fits and starts. In other words, the knee has to move smoothly. Another part of ‘gentle’ is safety and has to be taken in account during the design of the controller.
 - **Robust:** Applicable for different parameter settings, like the length of cables or the edge where the cables will aim at the knee. This has all to do with friction. Robustness will further be shown by a stable system with a possibility of a wide range of parameter differences during operation. Robustness is also necessary because of the interactive behave of the rehabilitation robot. The adaptable actuation will be force controlled.

2. Model

This chapter deals with the modelling of the knee joint. First of all, in paragraph 2.1, there is a description of the dynamic system modelled in an IPM. This IPM is converted in to a standard mechanical model, further simplified and presented by a block scheme in paragraph 2.2. The parameters for the models are determined in paragraph 2.3. Paragraph 2.4 deals with an adaptation of the model in relation to the real. This chapter ends with the adaptation of the 4th order model in paragraph 2.5.

2.1 Ideal Physical Model

The dynamic system, shown in figure 1.2, is converted in an Ideal Physical Model (IPM). An IPM is useful to describe a dynamic system in an orderly manner. In the case of the knee, two different domains were chosen: a rotation domain and a translation domain. The connection between these two domains takes place by means of transmissions. These transmissions are carried out by discs.

The IPM of the knee consists of:

- *Torque actuator*
- *Inertias* (motor-, gear axes-, disc1-, disc2 and knee inertia)
- *Mass of the Bowden cable*
- *Springs* (spring behaviour of the Bowden cable and spring to measure the applied force)
- *Dampers* (motor- and gear friction), friction in the cables and friction of the discs)

Figure 2.1 shows the IPM of the knee. The abbreviations in this IPM and the value of the parameters are listed in table 2.1.

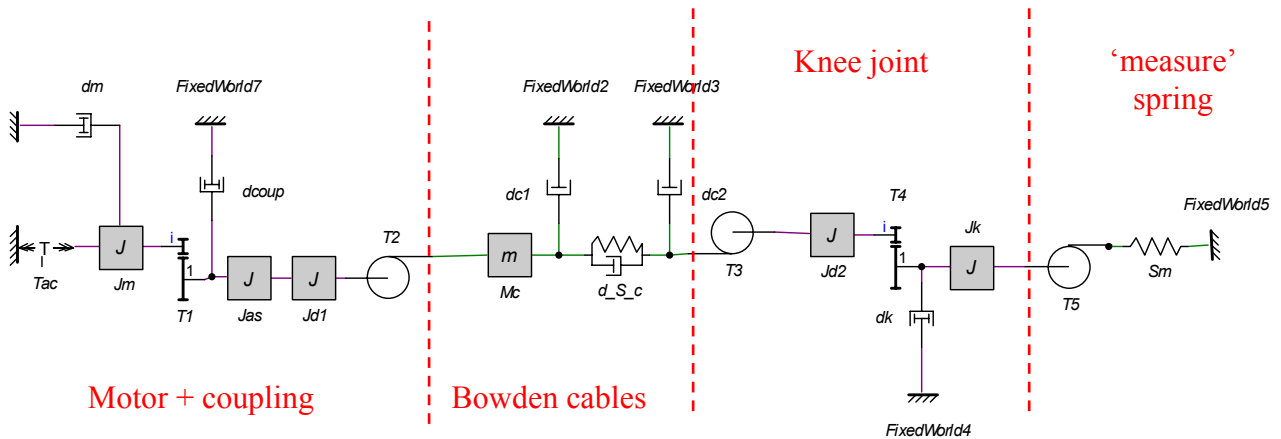


Figure 2.1: IPM of the dynamic system.

The Bowden cables in this system are represented as a mass – spring – damper combination. The applied force on the knee is measured by the ‘measure’ spring. The length of the ‘measure’ spring is used as a measure for the torque applied by the actuator to the knee. The length is measured by a Linear Variable Differential Transformer (LVDT).

2.2 Mechanical model

The IPM shown in figure 1 is converted in a mechanical model. This model is divided into two domains, namely, the ‘motor rotation domain’ and the ‘cable translation domain’. Firstly, the translations of masses and inertias to the motor rotation domain will be explained and after that the translations to the cable translation domain will be explained.

Translation to motor rotation domain

Firstly, the mass of the cable will be translated over transmission T_2 , as done in equation (2.1) Figure 2.2 shows the new situation.

$$J_{Mc} = Mc * T_2^2 \quad (2.1)$$

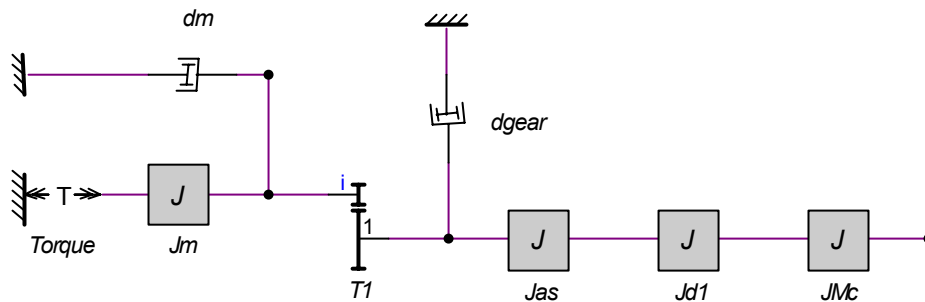


Figure 2.2: The situation after translation (2.1)

The three inertias are added and translated over T_1 to the motor rotation domain. The same is done for the friction caused by the gear. Equations (2.2), (2.3) and (2.4) shows these translations and addition. Figure 2.3 shows the motor rotation domain with the translated inertias.

$$J_{total1} = (J_{Mc} + J_{as} + J_{disc1}) * T_1^2 \quad (2.2)$$

$$J_{mtotal} = J_m + J_{total1} \quad (2.3)$$

The motor inertia is the dominant factor in J_{mtotal} : $J_{mtotal} \approx J_m$

$$dm_{total} = (d_{gear}) * T_1^2 + dm \quad (2.4)$$

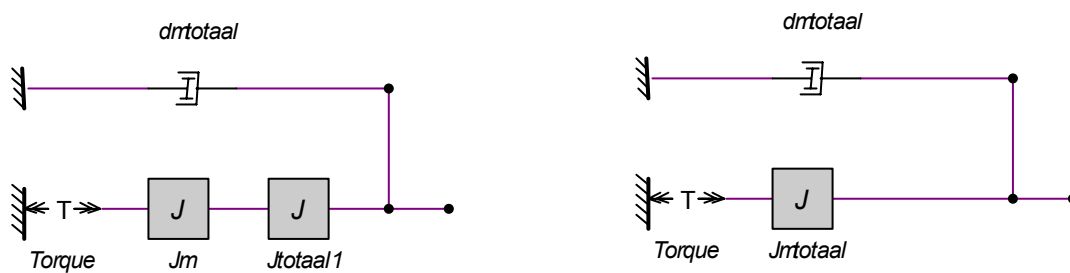


Figure 2.3: The situation after (2.2), (2.3) and (2.4)

Cable translation domain

Transmission T_4 is the transmission inside disc2 and has the value 1. This transmission is taken in account to get the IPM as complete as possible. In practice, the values of the knee inertia and the inertia of disc2 can be added without translation. The knee inertia has no effect on measurement results when the system is connected with the fixed world. The result is shown in figure 2.4.

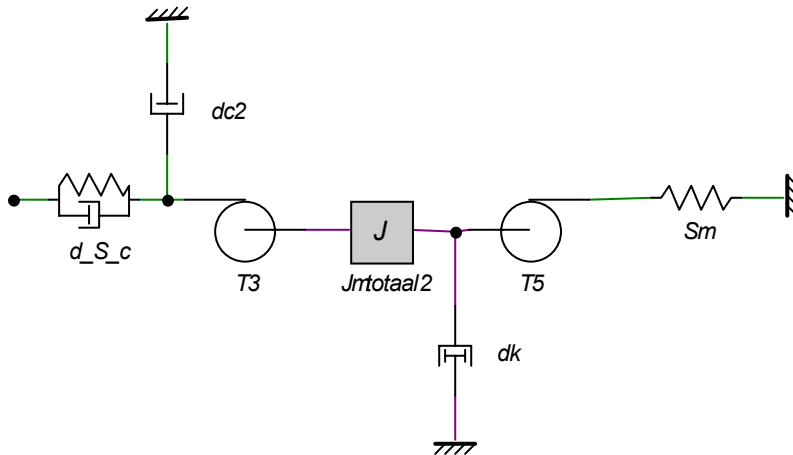


Figure 2.4: Situation after addition of the inertias of disc2 and knee

The inertia $J_{mtotaal2}$ and the friction d_k are translated over transmission T_3 to the cable translation domain. Equation (2.5) and (2.6) shown this translation. The transmissions T_3 and T_5 have the same value but are opposites. The measure spring S_m has the same value here as in the cable translation domain. Figure 2.5 shows the situation after the translations.

$$M_{totaal2} = J_{mtotaal2} * T_3^2 \quad (2.5)$$

$$d_{ktotaal} = d_k * T_3^2 \quad (2.6)$$

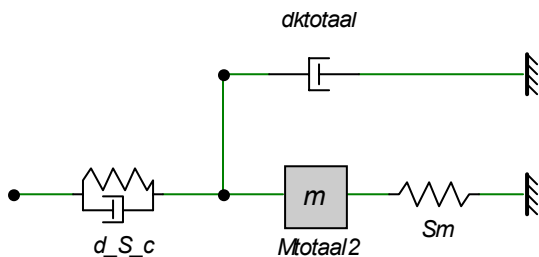


Figure 2.5: Situation after translations (2.5) and (2.6)

Both domains are linked up and gives the simplified mechanical model. It contains one inertia, one mass, two springs and a damper for both domains. It results in a 4th order system.

The simplified mechanical model is shown in figure 2.6.

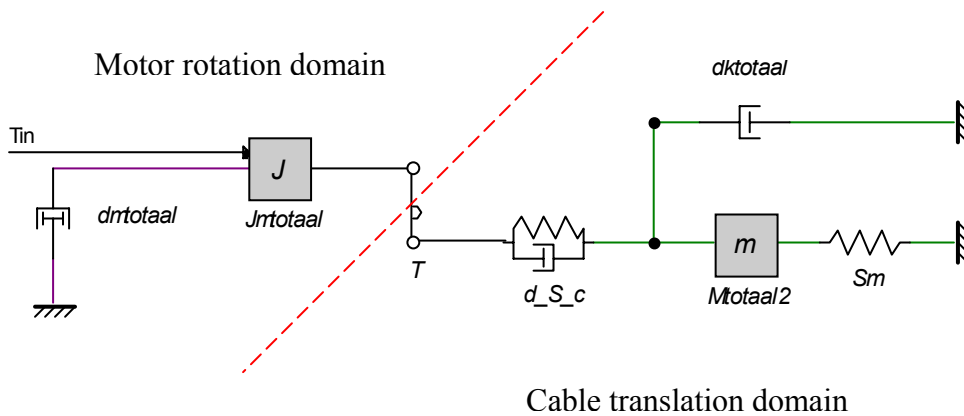


Figure 2.6: Simplified mechanical model

The control of, and the measurements on, the exoskeleton, especially the knee in this case, are done by using Matlab. This program is often used in control engineering related projects. Simulink is the tool for schematic modelling in Matlab. Simulink uses block schemes to represent a dynamic system.

The earlier developed simplified IPM (figure 2.6) is converted in a block scheme.

The converted IPM is shown in figure 2.7. The motor friction $d_{mtotaal}$ is divided in two motor frictions, the coulomb friction and viscous friction. This deviation is explained in the next paragraph.

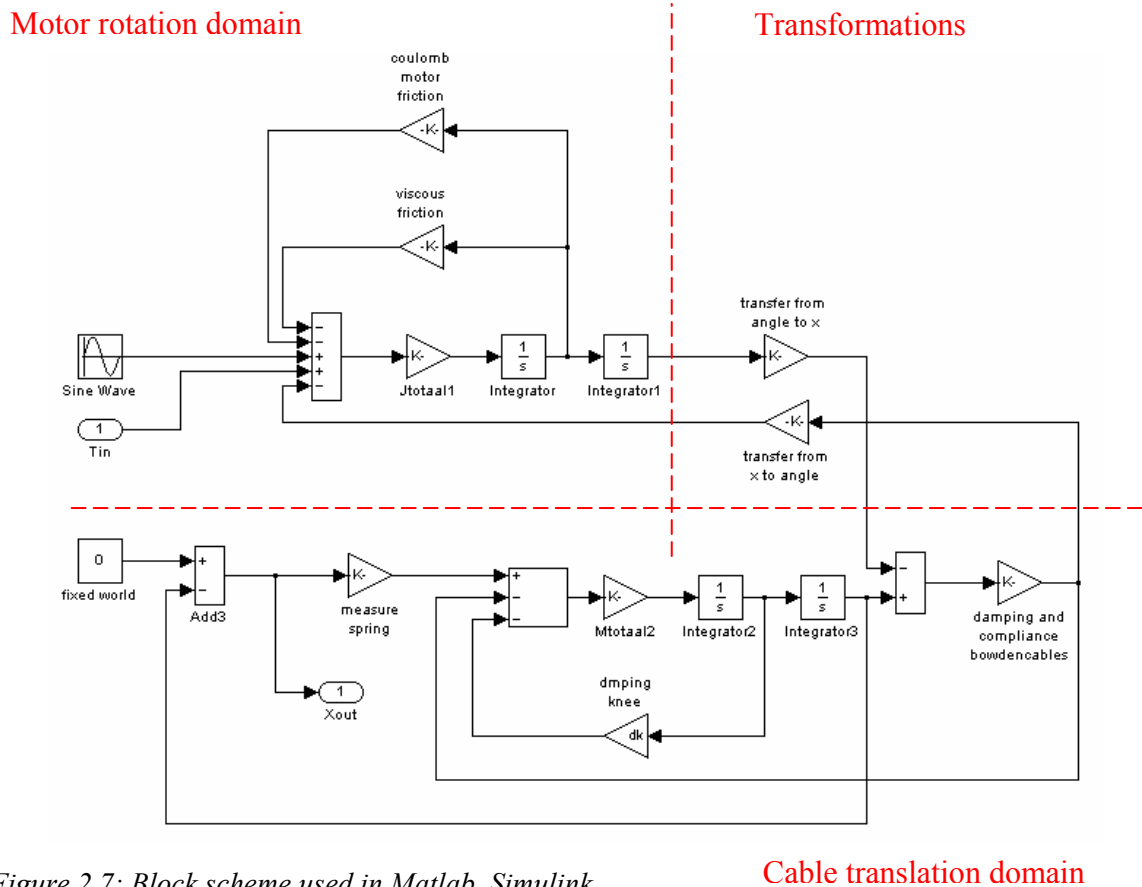


Figure 2.7: Block scheme used in Matlab, Simulink.

2.3 Parameters

After finishing the IPM, the different parameters are determined and listed in table 2.1. Some of the parameters, like spring constants or inertias are known from datasheets (see appendix A) but the friction of the motor in combination with the coupling is not available. The determination of the motor friction will be explained later on in this paragraph.

Transmissions	$T = out/in$	
T_1	1/8	Transmission motor – coupling
$T_2 = r1$	$31.12 \cdot 10^{-3}$	Transmission coupling – disc 1 (to Bowden cable)
$T_3 = r2$	$47 \cdot 10^{-3}$	Transmission cable – disc 2
T_4	1	Transmission inside disc 2
$T_5 = r2$	$47 \cdot 10^{-6}$	Transmission disc 2 – ankle/measure spring
Inertia's	$Kg \cdot m^2/rad$	
J_m	$160 \cdot 10^{-6}$	Motor inertia
J_{as}	$39 \cdot 10^{-6}$	Inertia of the motor axes
J_{d1}	$48.858 \cdot 10^{-6}$	Inertia of disc 1
J_{d2}	$361.555 \cdot 10^{-6}$	Inertia of disc 2
J_k	$47 \cdot 10^{-6}$	Inertia of the shin segment
Mass	Kg	
M_c	$150 \cdot 10^{-3}$	Mass of the Bowden cables
Friction	$Nm \cdot s/rad$	
D_m	$196.8 \cdot 10^{-3}$	Motor friction (par. 2.3)
D_c	$60 \cdot 10^{-3}$	Coupling friction (par. 2.3)
$dc1$	not known yet	Friction in the cable
$dc2$	not known yet	Friction in the cable
Spring	Nm	
D_{S_c}	150	Stiffness of the cable
S_m	$2 \cdot 90 \cdot 10^3$	Stiffness of the easure spring

Table 2.1: Parameters used in different schemes.

Motor friction

The motor and gearbox friction together are an unknown parameter. The two individual frictions known from datasheets are not reliable. The combination of the frictions is an important parameter. The motor and gearbox friction together are determined by a measurement. The motor and gearbox are connected to a pendulum by a belt, as shown in figure 2.8.

The angle of the pendulum and the time at which the pendulum stops swinging has to be measured. Three situations will be considered:

- (1) the pendulum in combination with the motor, coupling and the transmission belt
- (2) the pendulum and the transmission belt
- (3) the pendulum itself

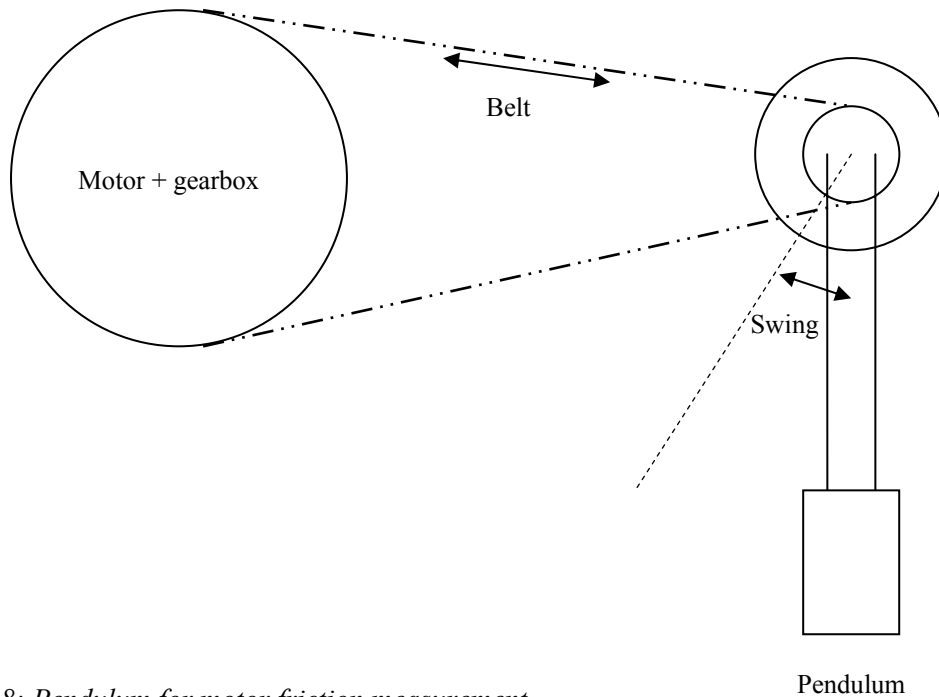


Figure 2.8: Pendulum for motor friction measurement

The three situations are modelled in 20-sim. 20-sim is a simulation program that can be used for control engineering. Figure 2.9 shows the model of the measurement situation.

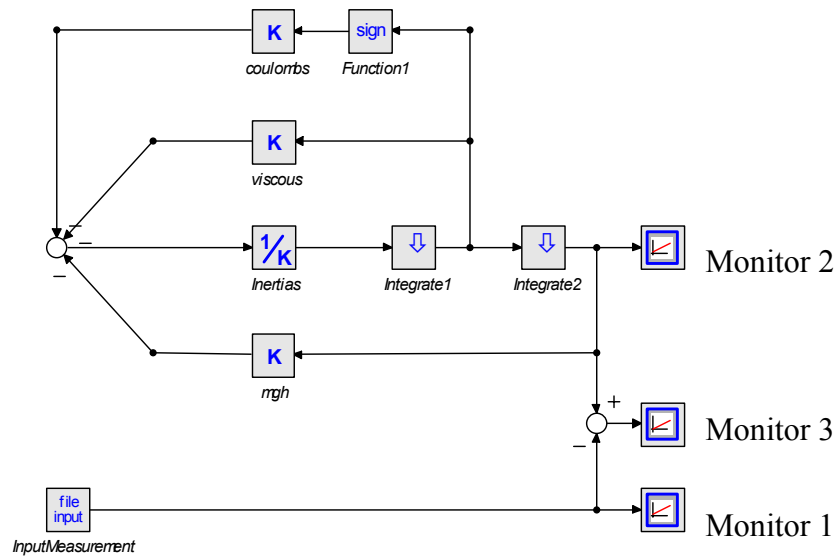


Figure 2.9: Model to compare the measurement outcome with the model outcome.

The model is useful for all three situations.

Monitor 3 in this model gives the differences between the signals of monitor 1 and monitor 2. Monitor 1 gives the signals from the data file of the measurements and monitor 2 gives the signals from the model.

The goal of this measurement is to match the model signals with the measurement signals. This goal is reached by changing the coulombs and viscous gains.

The program 20-sim contains a parameter optimising function. In this case the optimise function will optimise the coulombs and viscous friction in such a way that the simulation outcome matches the measurements as closely as possible.

The three measurements are done to estimate the frictions of the motor and belt. The total motor friction can be estimated by subtracting the parameters of situation (1) from situation (2). The friction of the belt can be estimated by subtracting the parameters of situation (3) from (2).

The parameters are translated to the motor domain. Table 2.2 shows the result of the optimising based on the measurements.

Situation	Description	Coulombs Nm.s/rad	Viscous Nm.s/rad
1	Motor + Belt + Pendulum	$240 \cdot 10^{-3}$	$61.3 \cdot 10^{-3}$
2	Belt + Pendulum	$0.272 \cdot 10^{-3}$	$8 \cdot 10^{-6}$
3	Pendulum	$16 \cdot 10^{-3}$	$56 \cdot 10^{-6}$
	Motor	$196.8 \cdot 10^{-3}$	$60 \cdot 10^{-3}$
	Belt	$1.2 \cdot 10^{-3}$	$24 \cdot 10^{-6}$

Table 2.2: friction parameters in different situations.

The important and necessary constant parameters are known. The only unknown parameter is the friction in the Bowden cables. This parameter depends on several things, like the velocity of the cable compared to the cover of the cable and the itinerary of the cable (mainly the amount of bends).

2.4 Measurements versus model

The measurements are done on the system shown in figure 2.5. The open loop situation of the knee is considered. The open loop transfer from motor current to LVDT – voltage is determined. The input of the model is the motor current and the output used for the feedback is the LVDT – voltage. This is why the open loop transfer is determined between these two points.

The bodeplot and the phase characteristic of the real dynamic system are found.

During this measurement the knee is connected with the fixed world. This means the knee is blocked and cannot move. The motor input is a torque and is presented by a multi sinus (multi sinus, a set of sinuses in the range from five to thirty Hertz) with a certain amplitude. The change of spring length is measured. The transfer of the motor current to the spring length is considered. The bodeplot is compared with the bodeplot of the model.

The aim is to find a model that behaves like the real dynamic system. The magnitudes of frictions are changed to find the best match with the real system and the model. The values of the gains represent the friction in the cables.

The coulombs motor friction is set to zero. This friction is sign depended but during the linearization of the model, this non-linear parameter is neglected. This parameter cannot be neglected during the design of the controller. For this reason, the viscous friction is increased to find the best match with the measurement.

Figure 2.10 shows the bodeplot and the phase characteristic of the measurement from five to thirty Hertz. Figure 2.11 shows the bodeplot of the model.

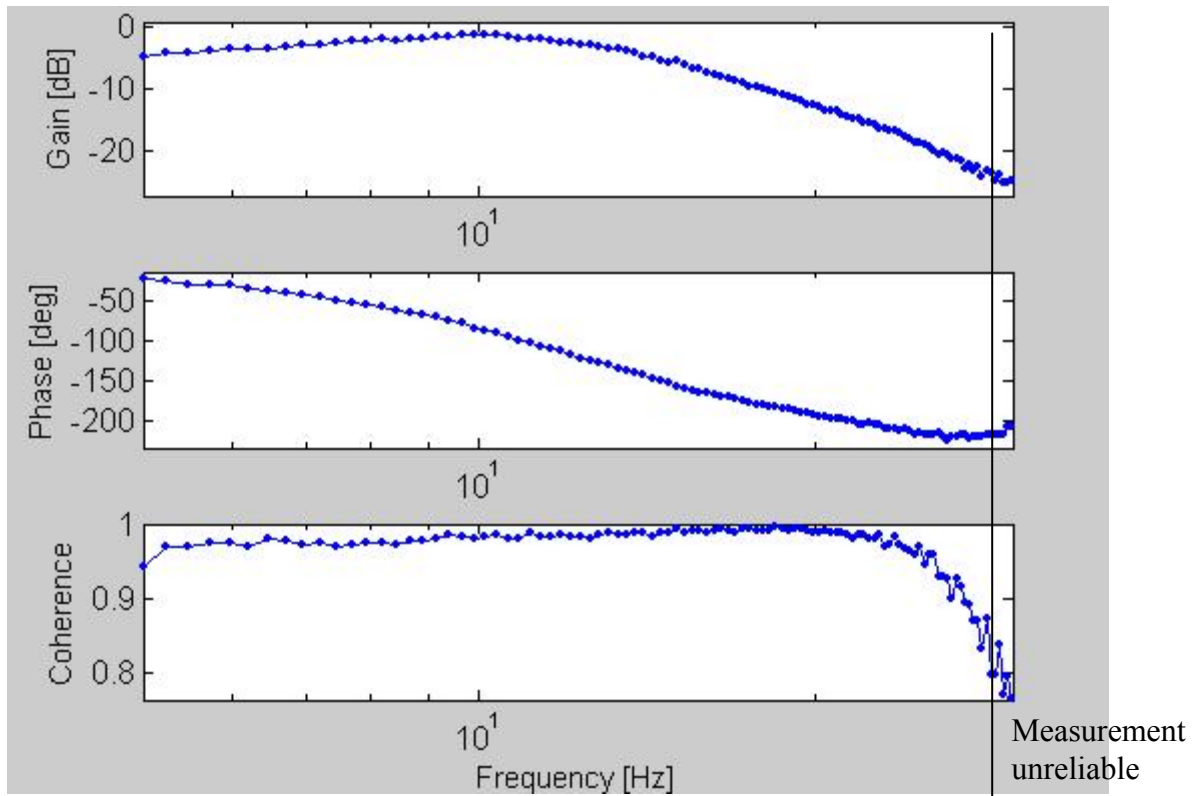


Figure 2.10: Bodeplot measurement, transfer from motor current to LVDT voltage

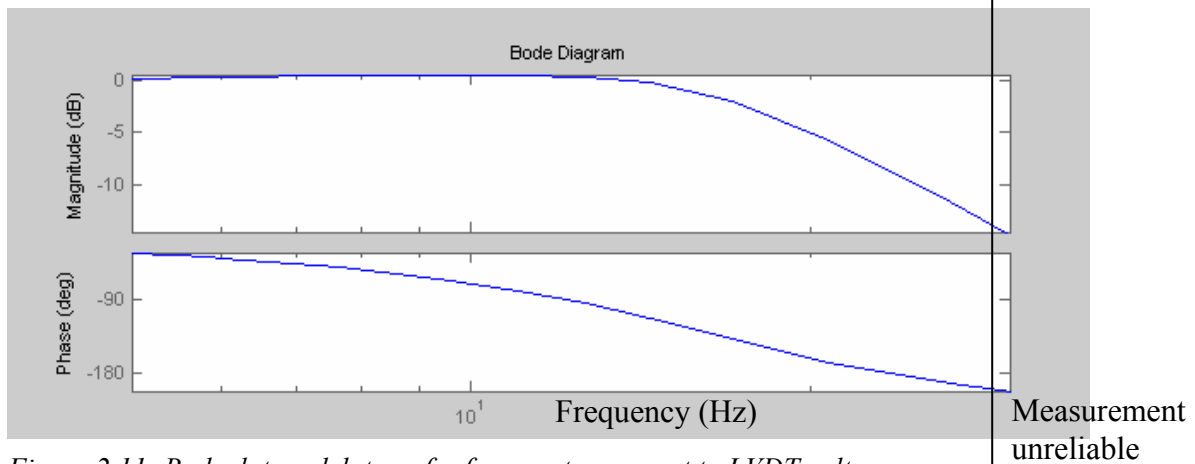


Figure 2.11: Bodeplot model, transfer from motor current to LVDT voltage

The matching of the model with the real system satisfies. Due to the small difference between the bodeplots and phase characteristics, further tuning of the gains for better results is not necessary.

The measurement is uncertain if the coherence of the plots is under 0.8 percent. This is the part right of the black line in figures 2.10 and 2.11.

The parameters as listed in table 2.1 are used. The used measure spring has a stiffness of $180 \cdot 10^3 \text{ N/m}$. Later on in this report, a measure spring with a stiffness of $70.6 \cdot 10^3 \text{ N/m}$ will be used.

2.5 Adaptation of the 4th order model

The relatively small value of $M_{\text{total}2}$ causes poles far from zero point of the real axis. These poles cause huge differences in the values of the A matrix but do not effect the relevant control bandwidth as well and could better be removed. Further, the huge differences give numerical problems as well, like singularity.

To solve this problem, the 4th order model shown in figure 2.6 is transformed in a 2nd order model. The mass and friction of the cable translation domain is translated to the motor rotation domain. Equation (2.7) and (2.8) gives these translations. The two springs are added in equation (2.9).

$$J_{Mc} = (M_c + M_{\text{total}2}) * T_2^2 * T_1^2 \quad (2.7)$$

$$dk_{\text{total}1} = dk_{\text{total}} * T_2^2 * T_1^2 \quad (2.8)$$

$$S_{\text{total}} = (d_{-S_{-c}} * S_m) / (d_{-S_{-c}} + S_m) \quad (2.9)$$

The 4th order system is converted in a 2nd order system after this translation. The mechanical model of this system is presented in figure 2.12.

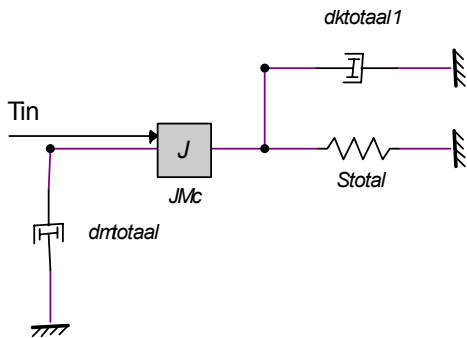


Figure 2.12: The 2nd order system after translations (2.7) and (2.8)

Figure 2.13 shows the block scheme of this model. The friction is presented here by a function. The function of the friction consists only of a viscous part. The coulombs friction is taken into account by increasing the viscous damping. The output of the system is the spring length X_{out} . To get this parameter, the force applied by the spring is divided by the stiffness of the measure spring.

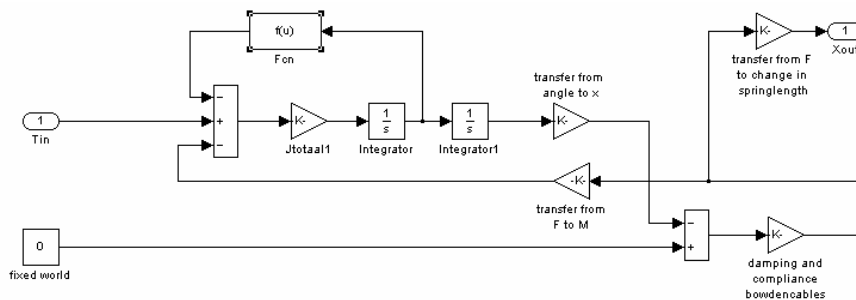


Figure 2.13: The 2nd order block scheme of the system

The system presented in figure 2.13 is used for further controller design. The next chapter deals with this topic.

3. Controller

This chapter deals with control system design of the knee joint. The first paragraph is used to explain the choice for LQG control. Paragraph 3.2 is used to make clear the operation of the LQG controller. Paragraph 3.3 deals with application of LQG in LOPES for the knee joint control and the discussion about the simulation results. This chapter ends with a paragraph about the parameter variation.

3.1 Choice of the controller

The models presented in chapter two are used to design the controller. The first step in control system design is to find an answer on the question: ‘which controller will be used’.

The answer depends on the specific properties and demands of the system. The system which has to be controlled in this case is the knee of the exoskeleton. The non-linear friction is a dominant property of the system. As mentioned in the goal description in chapter 1, the main demands of the controller are robustness and gentleness.

The system has non-linear parts due to the possible parameter variations and the coulomb friction. A robust controller is needed to handle this behaviour. State feedback control, like a PID controller, is an adequate mechanism to control systems with this uncertainty. A possible problem with the PID controller is the differential action ($\frac{du}{dt}$). The input signal can be noisy and can give problems during differentiation.

A model based controller is also a robust way to control systems with non-linear parts. The LQG controller is a model based controller, which makes estimations of the states to calculate the state feedback control gain. The advantage of a model based controller compared with a classic PID controller is the digital character and the complete mathematical formulation of the control mechanism.

Nevertheless, the PID can be used, although the LQG control algorithm contains some practical advantages, such as good estimations of the states. For this reason, the LQG controller will be used to control the dynamic system of the knee joint.

The LQG algorithm provides an optimal feedback for systems with deterministic parameters and takes in account the process disturbances and measurement noise.

The simplified IPM presented in figure 2.12 and the block scheme presented in figure 2.13 are used as starting point of the controller design. An optimal state feedback system can be defined when there is a well working state space representation of the system. Figure 2.13 is such a model and the optimal state feedback gain can be determined analytical, due to the Linear Quadratic theory. This method is called the Linear Quadratic Regulator (LQR).

The condition for using Linear Quadratic theory for the optimal state feedback is that all the states of the system are measurable. This is not always the case, or, sometimes, the measurements are disturbed by noise.

A good estimation of the states is necessary when one of those things takes place. There are several methods for estimating the states and one of them is also based on the Linear Quadratic theory. This is the Linear Quadratic Estimation or LQE.

These two methods can be combined in one control mechanism. The combination is LQG (e abbreviation of ‘Linear system with a Quadratic criterion and Gaussian noise’.) The two single methods (LQR and LQE) can be designed separately due to the eigenvalue separation

property of the LQG. This means that the poles (eigenvalues) of the combined system (LQG) consists of the union of the control poles (LQR) and the estimator poles (LQE).

The possibility to find an optimal state feedback system with the use of a well working state space model with a good estimation of the immeasurable states is the reason for using LQG to control the knee of the exoskeleton. A further work out of the LQG is given in the next paragraph.

3.2 Optimal LQG Control

The choice for a LQG control system is explained in paragraph 3.1. A further explanation of the LQG control method is given in this paragraph. Due to the eigenvalue separation property, the two single methods are explained separately. Figure 3.1 shows a system controlled by LQG control. Three parts can be distinguished; the system (indicated with (1)), the Linear Quadratic Regulator (indicated by (2)) and the Linear Quadratic Estimator (indicated with (3)).

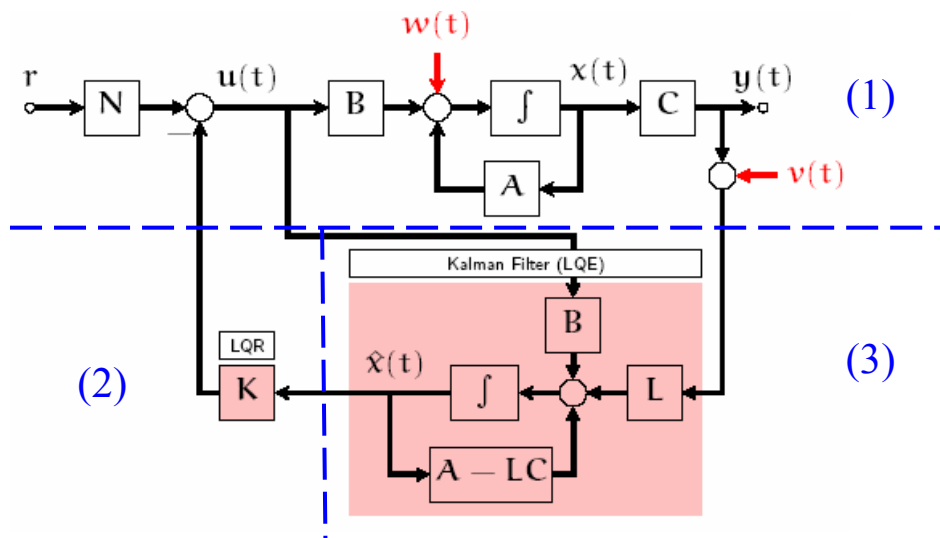


Figure 3.1: System controlled by a LQG controller

- LQR

The Linear Quadratic Regulator method can only be used when all the states in the system are influenced by the input signal. The demand for an optimal state feedback system is the controllability. This property will be checked first. Figure 3.2 shows an incomplete controllable system.

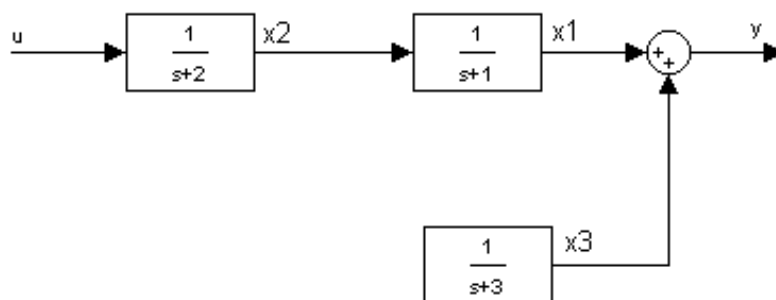


Figure 3.2: An incomplete controllable system

For the simple system in figure 3.2 is the controllability easy to determine. For more complex systems, the use of a pc is indispensable. Matlab is used to check the controllability of the knee joint. The dynamic system of the knee joint is controllable.

When the system is controllable, the optimal feedback gain can be found as followed:

$$1) \text{ Find the system description } \rightarrow \begin{cases} \dot{x} = Ax + Bu \\ y = Cx + Du \end{cases} \quad (3.1)$$

When $C = I, D = 0$ and $u = Kx$ (see figure 3.3), the equation of the total system can be simplified to:

$$\dot{x} = (A + BK)x \quad (3.2)$$

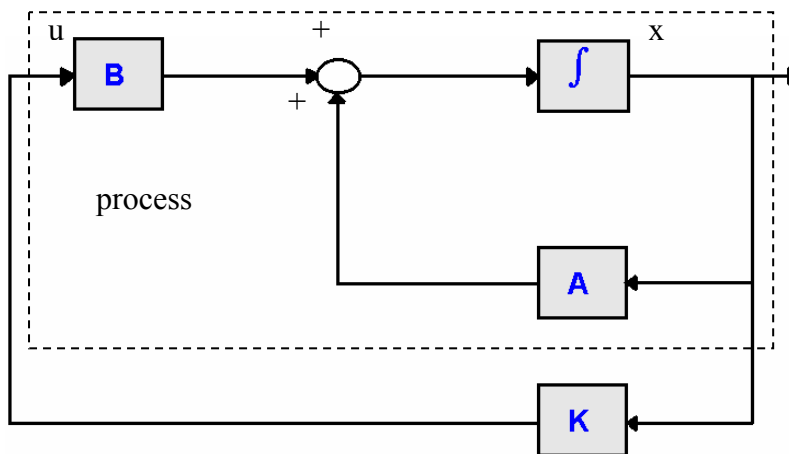


Figure 3.3: Process with full state feedback

- 2) To find the optimal value of K , a criterion has to be defined. This system uses the quadratic criterion which is defined as:

$$\begin{aligned} J &= \int_0^{\infty} (x^T Q x + u^T R u) dt \\ &= \int_0^{\infty} (x^T (Q + K^T R K) x) dt = \int_0^{\infty} (x^T (Q'') x) dt \end{aligned} \quad (3.3)$$

The matrix Q is a weight matrix for the system noise, the matrix R for the measurement noise. Both matrices have to be determined manually. The choice for Q and R is a trade-off between control performance (Q large) and low input energy (R large). Only the relative values of Q and R are relevant. The Q and R matrices need to be tuned until satisfactory behaviour is obtained.

- 3) The last step is to find parameters which influence the value of the criterion (K). This can be done by noting the integrand of the criterion as a derivation of a Liapunov function:

$$x^T (Q + K^T R K) x = -\frac{d(x^T P x)}{dt} \quad (3.4)$$

Now there is a relation between the two unknown parameters K and P and the given parameters A, B, Q and R.

Q is a symmetric positive definite matrix if all the elements of K are unequal. After some mathematics (derivation of $x^T P x$ and a further workout of (3.4)) gives the Ricatti equation:

$$A^T P + PA + Q + K^T B^T P + PBK + K^T RK = 0 \quad (3.5)$$

When (3.5) is satisfied, the feedback system is due to Liapunov global asymptotic stable. This means that $x \rightarrow 0$ for $t \rightarrow \infty$.

The criterion can now be rewritten to

$$J = x^T(0)Px(0) \quad (3.6)$$

There is an extreme value for criterion J when the values of K are:

$$\frac{\partial J}{\partial k_{ij}} = \frac{\partial P}{\partial k_{ij}} = 0 \quad (3.7)$$

To fill (3.6) and (3.7) into (3.5), (3.5) can be rewritten to:

$$2 \frac{\partial K^T}{\partial k_{ij}} B^T P + 2 \frac{\partial K^T}{\partial k_{ij}} RK = 0 \quad (3.8)$$

The terms $\frac{\partial K^T}{\partial k_{ij}}$ are equal to 0 or 1. (3.8) is true if

$$B^T P + RK = 0 \quad (3.9)$$

The solution for K is:

$$K = -R^{-1} B^T P \quad (3.10)$$

(See for a detailed description [2])

This K is the optimal state feedback gain used in the LQR control system

The basic model of a LQR controlled system is given in figure 3.4. In this model $w(t)$ is the system noise and $v(t)$ the measurement noise.

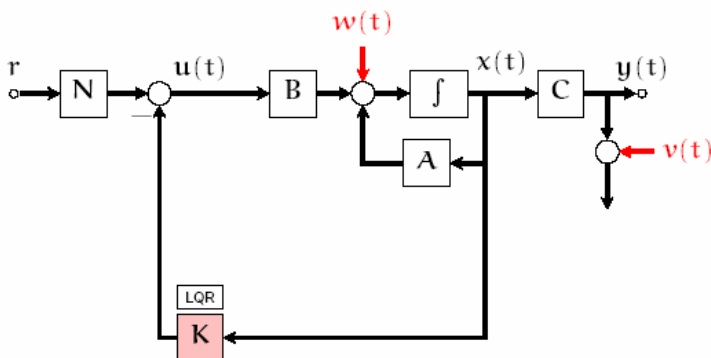


Figure 3.4: Basic model of a LQR controlled system

[4] gives a detailed description to find the optimal K.

- LQE

The Linear Quadratic Estimator mechanism is used when not all states of a system are measurable. Before LQE can be used, the ‘observability’ of the system has to be checked. A system is observable if *all* states influence the output. Figure 3.5 gives a system which is not complete observable.

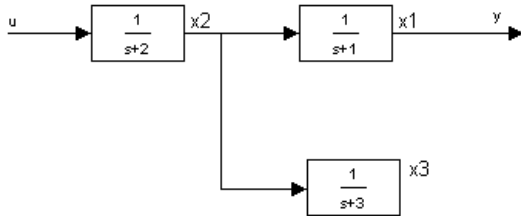


Figure 3.5: A not completely observable system

Matlab is used to check the observability of the system. It turns out the system is observable. When the system is observable, the optimal observer can be designed. An example of an optimal observer is the Kalman filter. Figure 3.6 shows a system with a Kalman filter. To estimate the states in an optimal way is to determine the feedback matrix L optimal. The L matrix can be determined analytical and uses also the matrices Q and R as described under the LQR control mechanism.

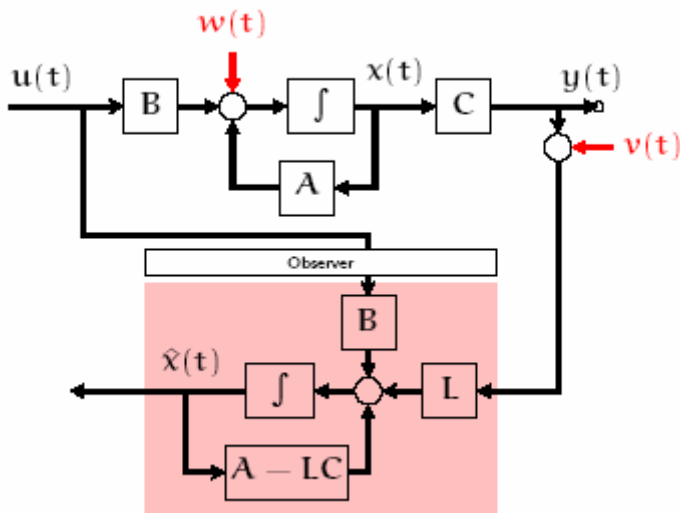


Figure 3.6: Basis system with Linear Quadratic Estimator (Kalman filter)

The procedure to find the values of the L matrix is as followed:

- 1) The system noise and the measurement noise are assumed as white noise sources. The magnitude of this noise signals are noticed with the Q and R matrices. Q and R are covariance matrices, $Q = E(w w^T)$ and $R = E(v v^T)$.
- 2) Figure 3.5 actually shows two processes; the system and the observer. This results in two process descriptions:
 - the process disturbed by noise:

$$\begin{aligned}\dot{x} &= Ax + Bu + Gw \\ y &= Cx + v\end{aligned}\tag{3.11}$$

- and the observer:

$$\begin{aligned}\dot{\hat{x}} &= A\hat{x} + Bu + L(y - \hat{y}) \\ \hat{y} &= C\hat{x}\end{aligned}\tag{3.12}$$

3) The error in the states are:

$$\begin{aligned}\dot{e} &= Ax + Bu + Gw - A\hat{x} - Bu - L(Cx + v - C\hat{x}) \\ &= (A - LC)e + Gw - Lv\end{aligned}\tag{3.13}$$

4) The value of the feedback matrix L is given by the equation:

$$L = CPR^{-1}\tag{3.14}$$

The P in (3.14) is the solution of the Riccati equation

$$AP + PA^T + GQG^T - PC^T R^{-1} CP = 0\tag{3.15}$$

3.3 LQG used in LOPES (simulation results)

This paragraph deals with the LQG mechanism used in LOPES to control the knee joint. The used schemes are first discussed. The second part of this paragraph deals with the simulation results.

Figure 3.7 shows the overall control scheme with the LQR and LQE algorithms. This is the LQG used in LOPES to control the knee joint.

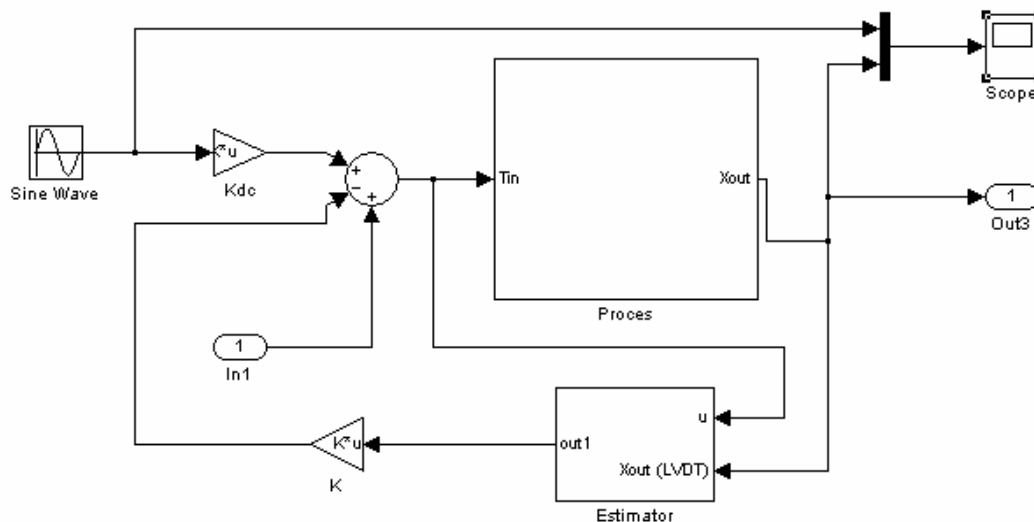


Figure 3.7: The control scheme for the knee joint, using LQG

The input is a sine wave and simulated the applied torque on the system. K_{dc} is the parameter, used to cancel the DC gain of the open loop system. The process contains the block scheme as shown in figure 2.13. The output is X_{out} , which is also the LVDT output that gives the change in spring length.

This output, combined with the input of the process, is the input for the estimator. The output is a matrix with the states for the LQR gain. Figure 3.8 shows the estimator block scheme.

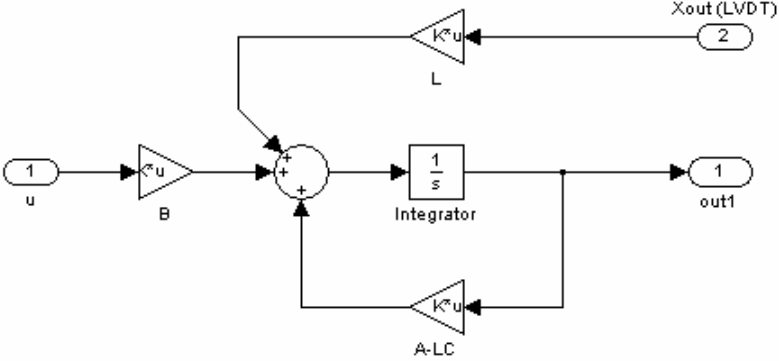


Figure 3.8: The estimator of the system

The optimal feedback is found to use the LQR function in Matlab

The scheme in figure 3.7, with the subsystems in it and the mathematical functions in Matlab gives a well working LQG controller.

This controller is ready for simulation.

The matrices Q , R and for the LQR algorithm are defined first. The optimal magnitude is found by trial and error. The Q and R matrices have to be tuned so that an acceptable error appears together with realistic torque commands. The Q matrix is a 4x4 matrix, the dimension of the Q matrix has the same dimension as the A matrix of the system. The dimension of the R matrix is dependant of the amount of outputs of the system (the number of rows of the C matrix). The matrices are:

$$Q = \begin{bmatrix} 1 & 0 \\ 0 & 0 \end{bmatrix} \quad R = [10 * 10^{-3}]$$

The choice for this matrix Q means that only the first state (q_{11}) is used to minimise the cost function J as presented in equation (3.3).

The matrices Q , R and G for an optimal estimation of the states (LQE) are defined in the same manner as for the LQR and are:

$$Q = [1] \quad R = [1 * 10^{-6}] \quad G = [1 ; 0.5]$$

The covariance Q represents the magnitude for the noise on the states and the covariance R the measurement noise. The dimension of Q must be square with as many columns as G . The variance P in the error equation (3.13) has to be minimized to find the conditions in the course

of which the derivation of P is zero. These conditions give the optimal value for L . G is the weighting matrix for the noise on the states.

Figure 3.9 shows the response of the open loop system. The system is simulated with the knee connected with the fixed world, like the models in chapter 2. The input signal is a sine wave with an amplitude of 0.001. This agrees with the real movement in this situation, which is a movement with a magnitude of 1 millimetre.

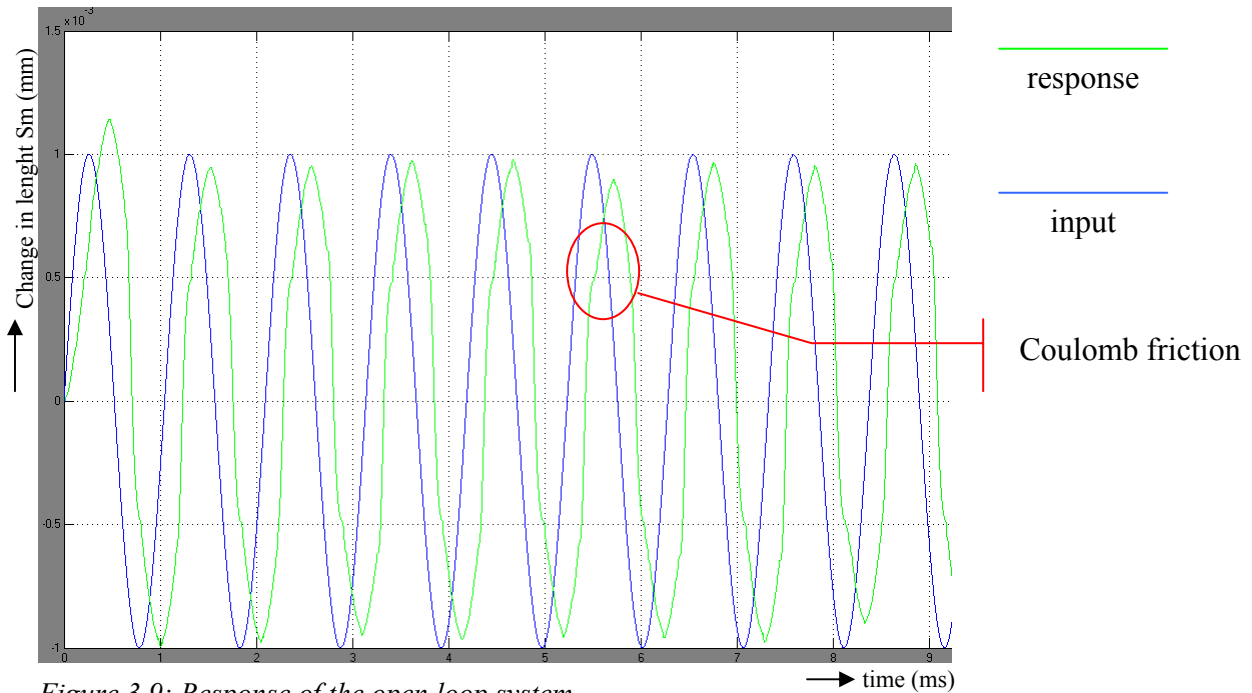


Figure 3.9: Response of the open loop system

The response of the open loop system starts with an overshoot and continues in an irregular course. The irregular form of the response and the damping in the system is caused by the coulombs friction in the system. There is a (reasonable) time delay too, which should not be neglected.

Figure 3.10 shows the response of the system controlled by the designed LQG algorithm.

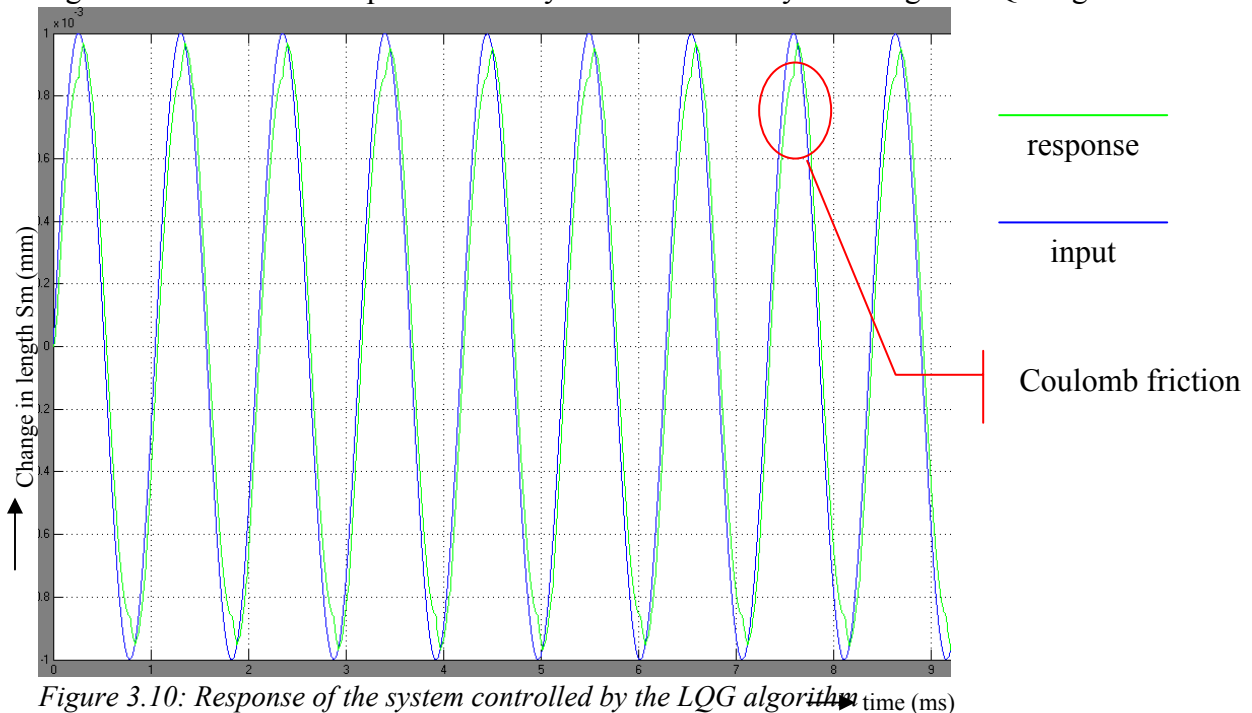


Figure 3.10: Response of the system controlled by the LQG algorithm

The response of the controlled system is much better compared to the open loop behaviour. The time delay now is smaller than 0.01 and is negligible in the operating range of this system (around 4 Hz). The irregular course of the magnitude of the response has disappeared. There is only a little distortion at the turning points and a little damping in the output of the system.

The transfer from system reference to system output of the controlled closed system is given in figure 3.11. It shows a stable system without overshoot for the relevant frequency range.

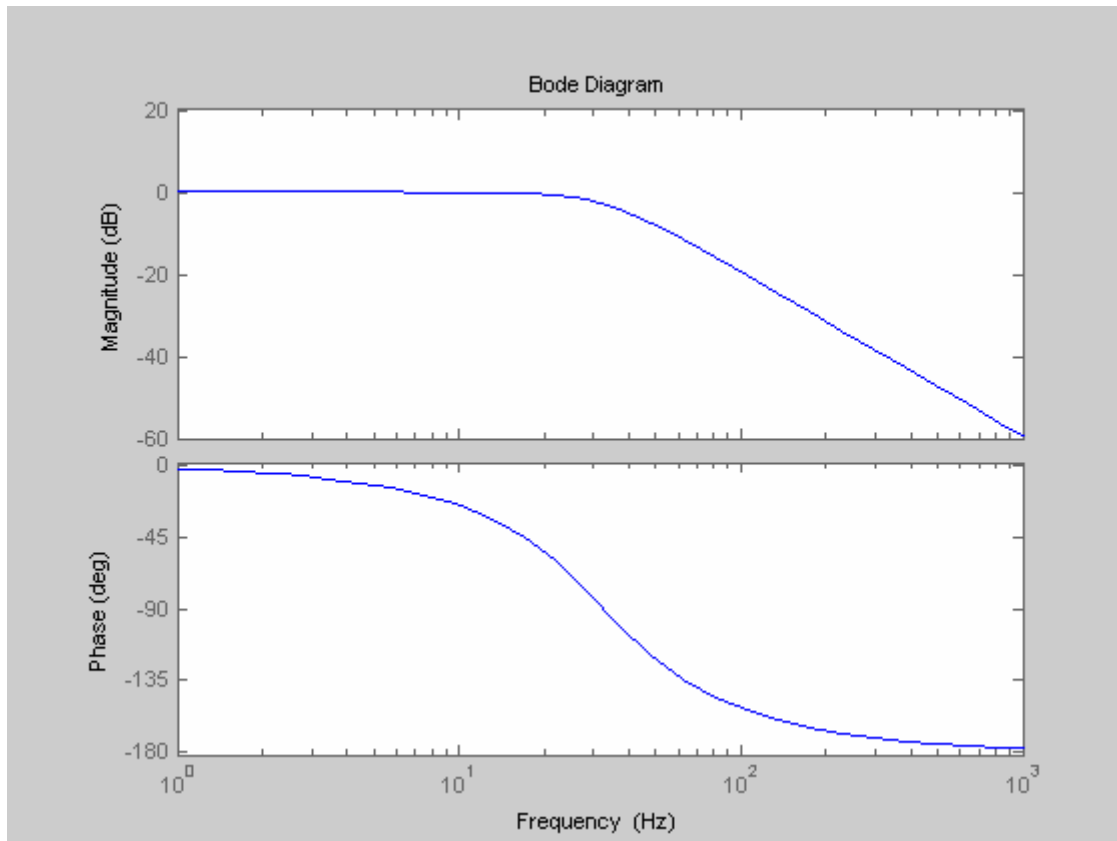


Figure 3.11: Bodeplot of the controlled closed loop system

3.4 Parameter variation

The chosen parameters give a well working controller for the specified friction as shown in the previous paragraph. This paragraph deals with the parameter variation. Some of the parameters are changed, but the controller settings are kept the same. The possible changing parameters for this system are the coulomb and viscous friction. Variation of other parameters during operating, like the motor inertia, is not plausible.

The aim of the parameter variation is to find the borders of the controller in which the controller can operate satisfactory.

First the friction will be set on zero. The output of the LQG controlled system follows the input exactly as expected. This is shown in figure 3.12.

The uncontrolled or open loop system gives some more disturbances in the output signal. This is caused by the total stiffness of the added springs. Figure 3.13 shows the output of this open loop system.

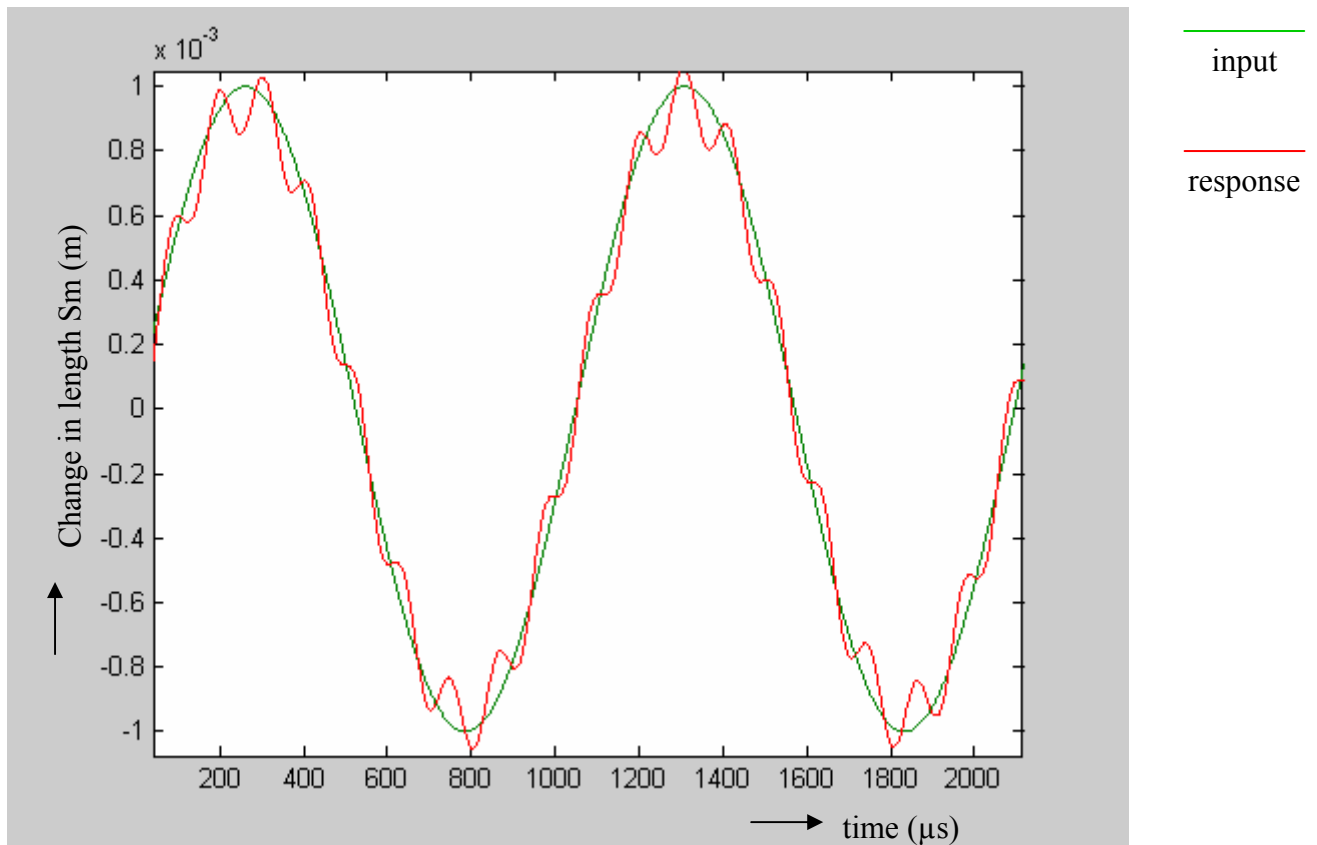


Figure 3.12: Response of open loop system without friction

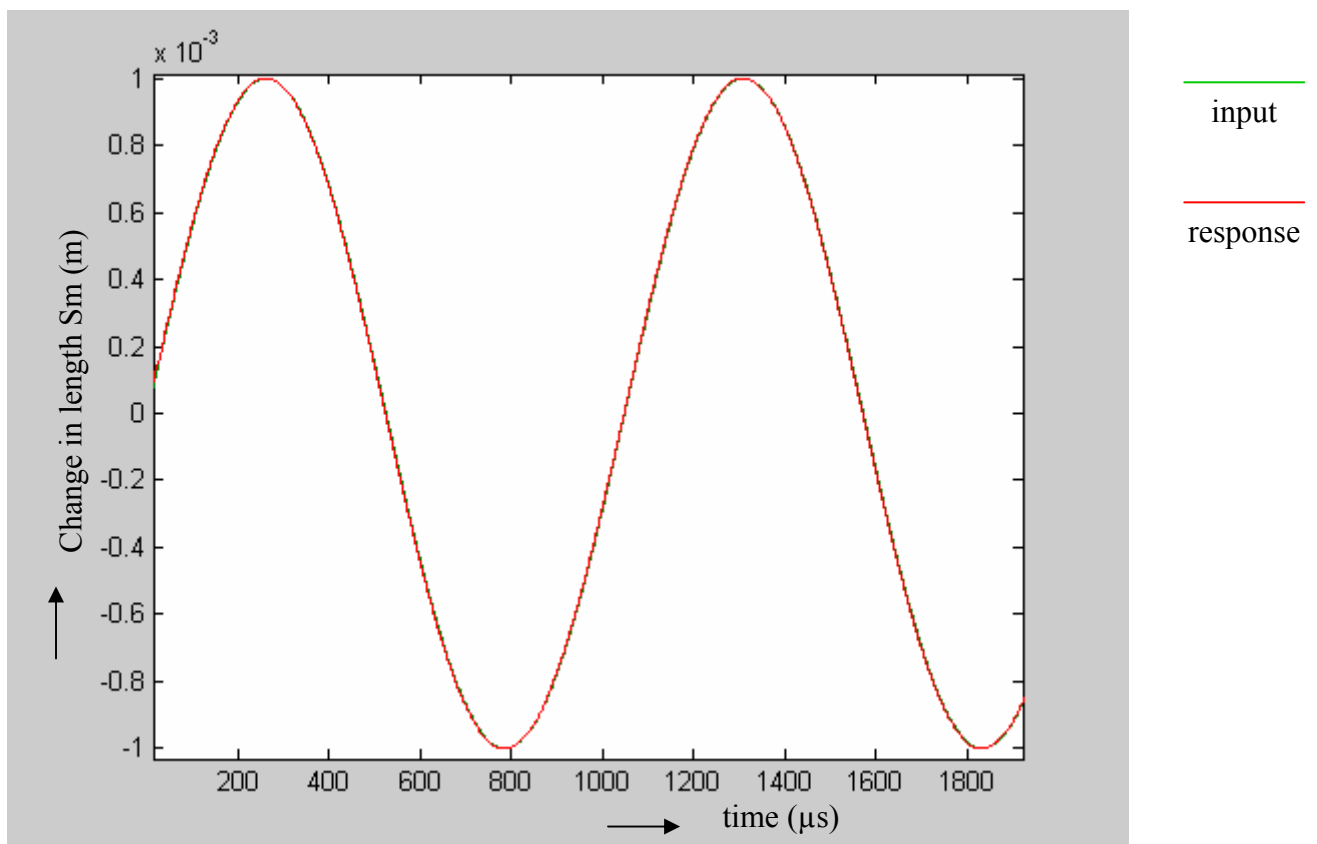


Figure 3.13: Response of the closed loop (controlled) system without friction

The coulomb friction can rise with a number of 380% compared to the friction as used during controller design. This percentage is only valid without changing the viscous damping. The viscous friction can rise with a number of 3420%, also in comparison with the viscous friction during controller design and without changing the coulombs friction. These values are only theoretical possible. The force commands become unrealistically high values by this friction raise.

If the coulomb and viscous friction both increase with 220% will the open loop system has a response as shown in figure 3.14. The response of the system matched not with the reference signal. The output form becomes a sawtooth wave in stead of the sine reference signal.

The closed loop (controlled) system are kept stable and controllable by the same friction rise. Figure 3.15 shows the response with the friction increased with 220%. The output of the system follows the reference signal with a small delay (<0.02%).

The rise of 220% for both frictions influences the value and form of the friction. The friction behaves as a sine wave under normal conditions. The friction behaviour changes from sine wave into block form, due to the friction rise of 220%. This block form is shown in figure 3.16.

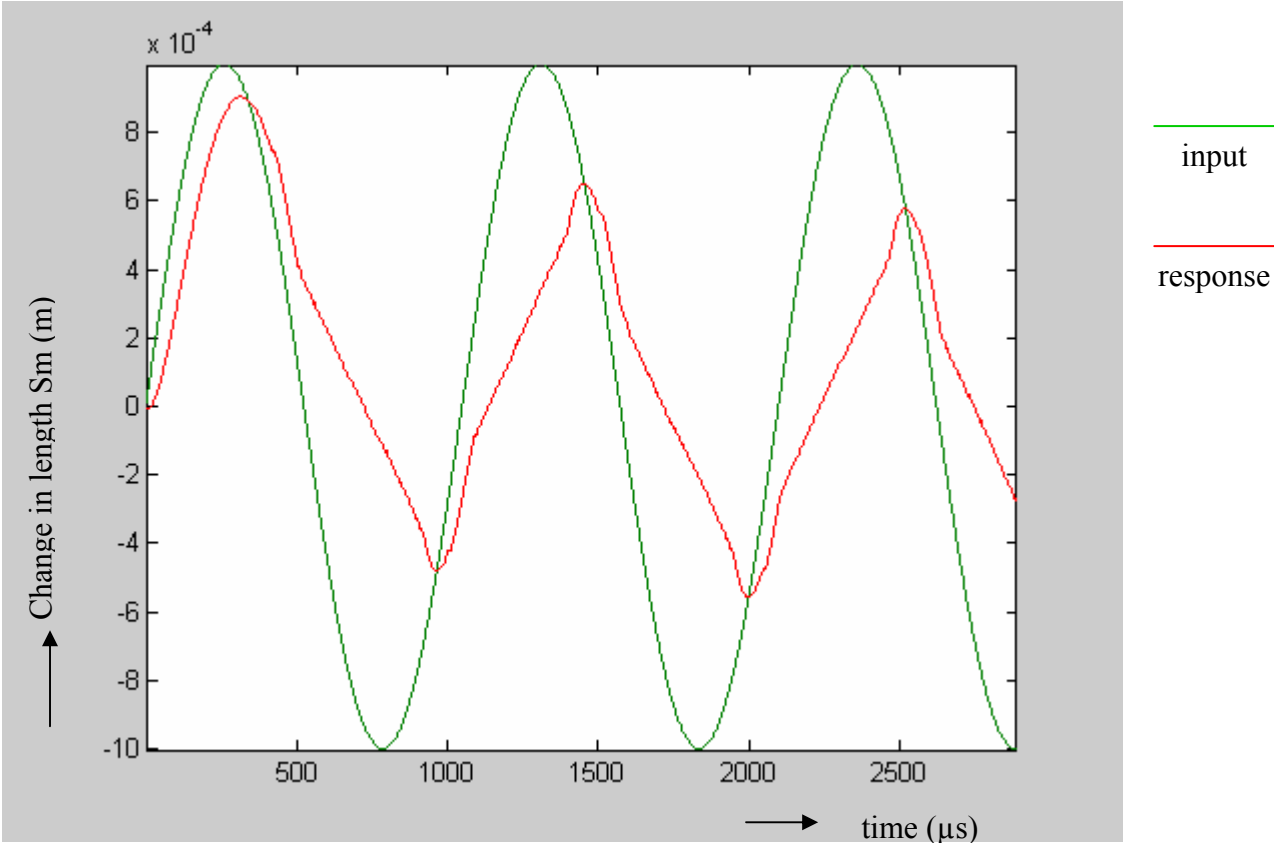


Figure 3.14: Response of the open loop system by a friction rise of 220%

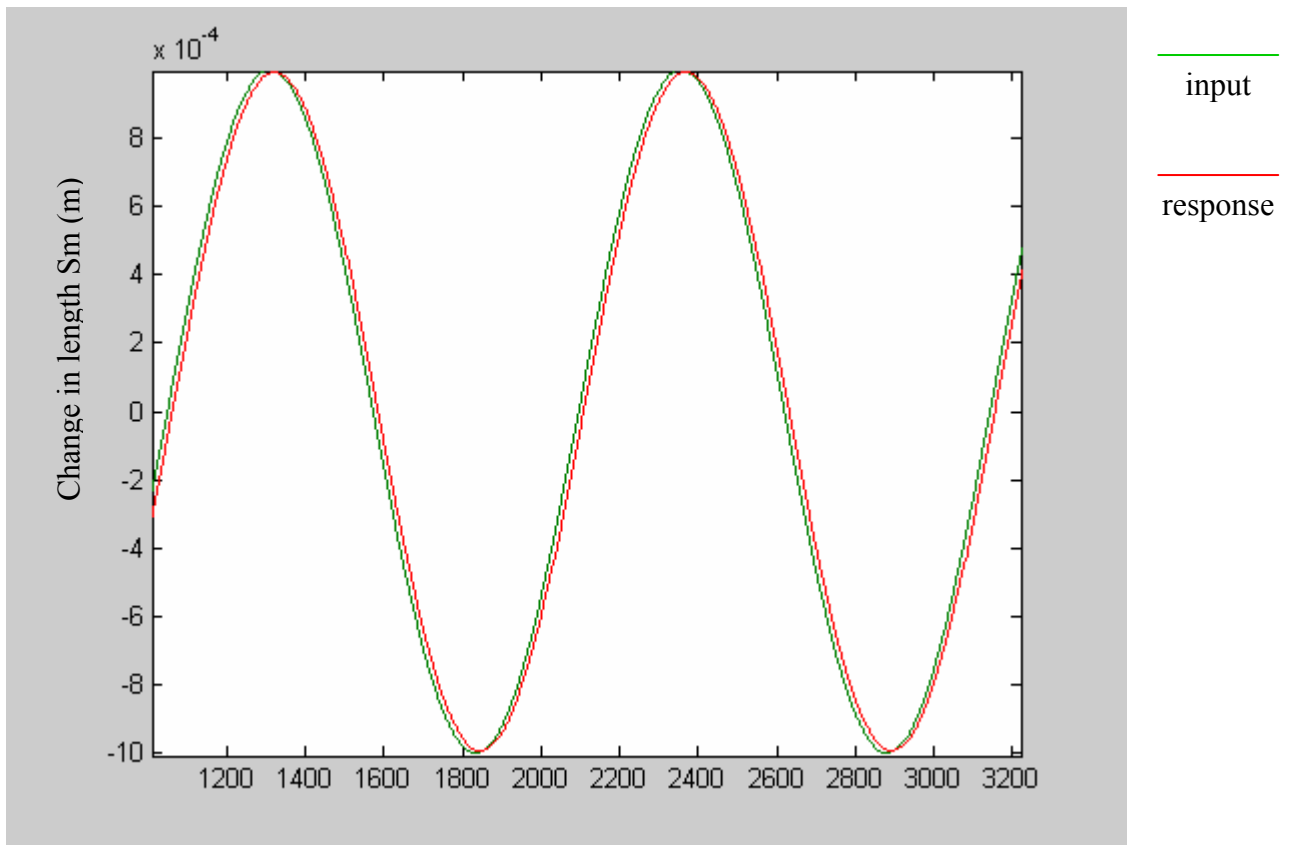


Figure 3.15: Response of the closed loop system by a friction rise of 220%

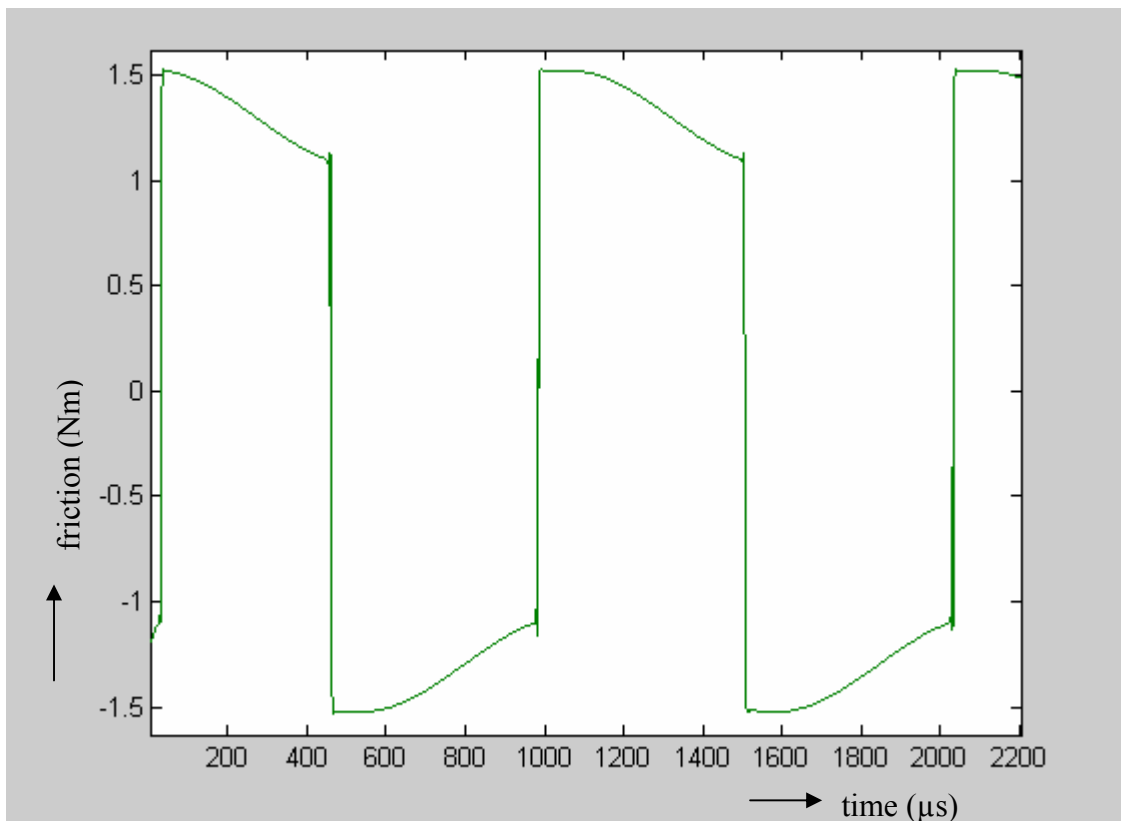


Figure 3.16: The friction by a rise of 220%

The LQG controller is tested enough for using it in practice, on the exoskeleton. This experiment is described in the next chapter, chapter 4.

4. Test results

This chapter deals with test results of the designed controller. In the first paragraph the model used in chapter 3 is adapted, because the measure spring in the system has changed. Paragraph 2 deals with the results of the tested controller.

4.1 Transfer open loop system with new parameter

The measurements and simulations in this report are carried out on the system as described in chapter 2. The used measure spring in this system has a stiffness of $180 \cdot 10^3 \text{ N/m}$. This is a relatively large stiffness and this causes a small change in spring length. The change in spring length will increase by using a spring with less stiffness. More spring length means a more sensitive system. The disadvantage of less stiffness is a lower bandwidth for a larger amplitude. For this reason, the stiffness of the measure spring is decreased from $180 \cdot 10^3 \text{ N/m}$ to $70.6 \cdot 10^3 \text{ N/m}$. This new parameter gives a new transfer function and open loop behaviour.

The procedure described in paragraph 2.5 is also used here to match the model with the measurement. Figure 4.1 shows the bodeplot of the measurement of the open loop transfer from motor current to LVDT voltage.

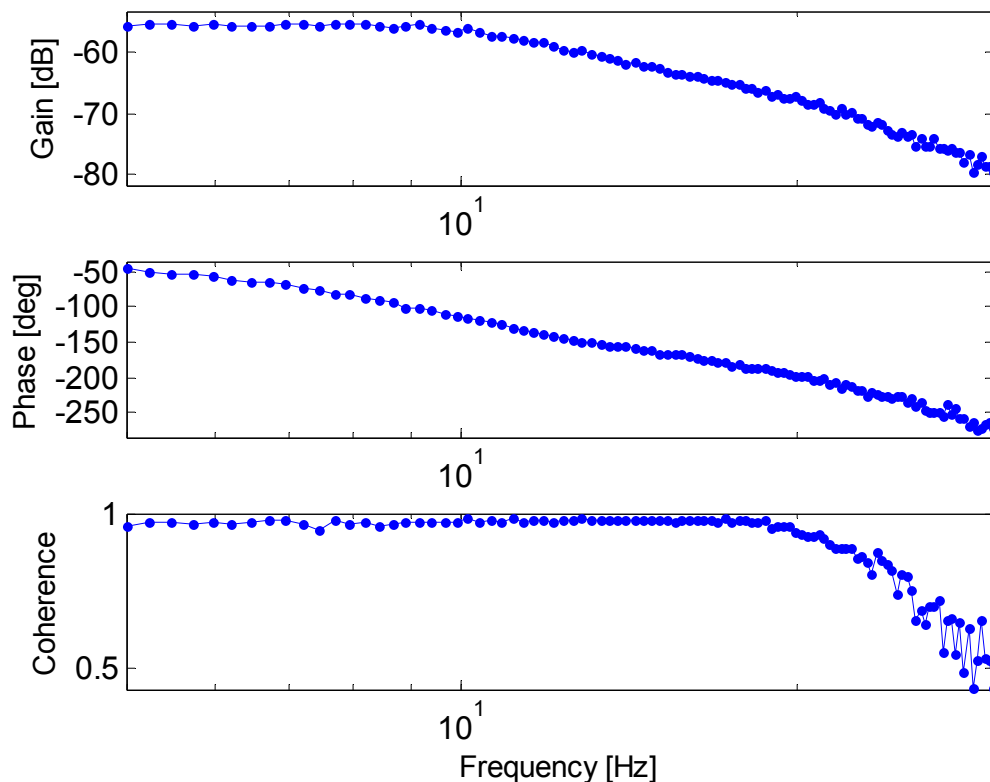


Figure 4.1: Transfer of open loop system from motor current to LVDT voltage

The transfer function of system is estimated by Matlab. Equation (4.1) gives the transfer function of the system. The open loop transfer of the bodeplot goes from motor current to LVDT length. The transfer of the function goes from motor torque to LVDT – length. The

gain in the transfer function is the factor between the controlled motor current and the motor torque.

$$H = \text{gain} * \frac{\frac{1}{m}}{s^2 + \frac{d}{m} \cdot s + \frac{k}{m}} * e^{-s(t_{\text{delay}})} = \frac{5.865}{s^2 + 63.1 \cdot s + 4072} * e^{-s(0.007)} \quad (4.1)$$

The stiffness of the system is supposed to be known and is used to calculate the mass in the system from the last part of the denominator of (4.1). This calculated mass differs a factor 1.1 of the mass determined in the previous chapters. This difference in the mass can be caused by the value of the total stiffness in the system. The value of the stiffness of the newly used springs ($70.6 \cdot 10^3 \text{ N/m}$) are taken from the datasheets. The real stiffness of the springs are not measured and can differ a little from the datasheet value.

The damping can be calculated by $\frac{d}{m} = 65.01$. Figure 2.13 is adapted with the new parameters and the bodeplot of the model and figure 4.1 is exactly the same. The new parameters for this system are:

Mass	$1.7839 \cdot 10^{-4}$	gain	70
damping	$11.6 \cdot 10^{-3}$	t_{delay}	0.007

A new LQG controller is designed with these parameters. The matrices for LQR (Q and R) and LQE (Q, R, and G) are the same as those described in paragraph 3.3. The new controller is calculated as described in chapter 3.

4.2. Test results

The newly calculated controller, as described in the previous paragraph, is simulated by a model and tested on the exoskeleton. This is done to verify the used models and to test the controller in practice. It is important to find out the closed loop behaviour of system, compared with the simulated closed loop behaviour.

The new LQG controller is tested on the system connected with the fixed world. As mentioned earlier in this chapter, the values of the different matrices, used in the controller are calculated from the system described in the paragraph 3.

The optimal gain values are:

$$K = [9.2999 \quad 0.0472]$$

The values of the L matrix are:

$$L = \begin{bmatrix} 0.0418 \\ -1.3225 \end{bmatrix}$$

First of all comes the closed loop transfer from reference to LVDT – voltage, simulated for a model without time delay. Figure 4.2 shows this bodeplot.

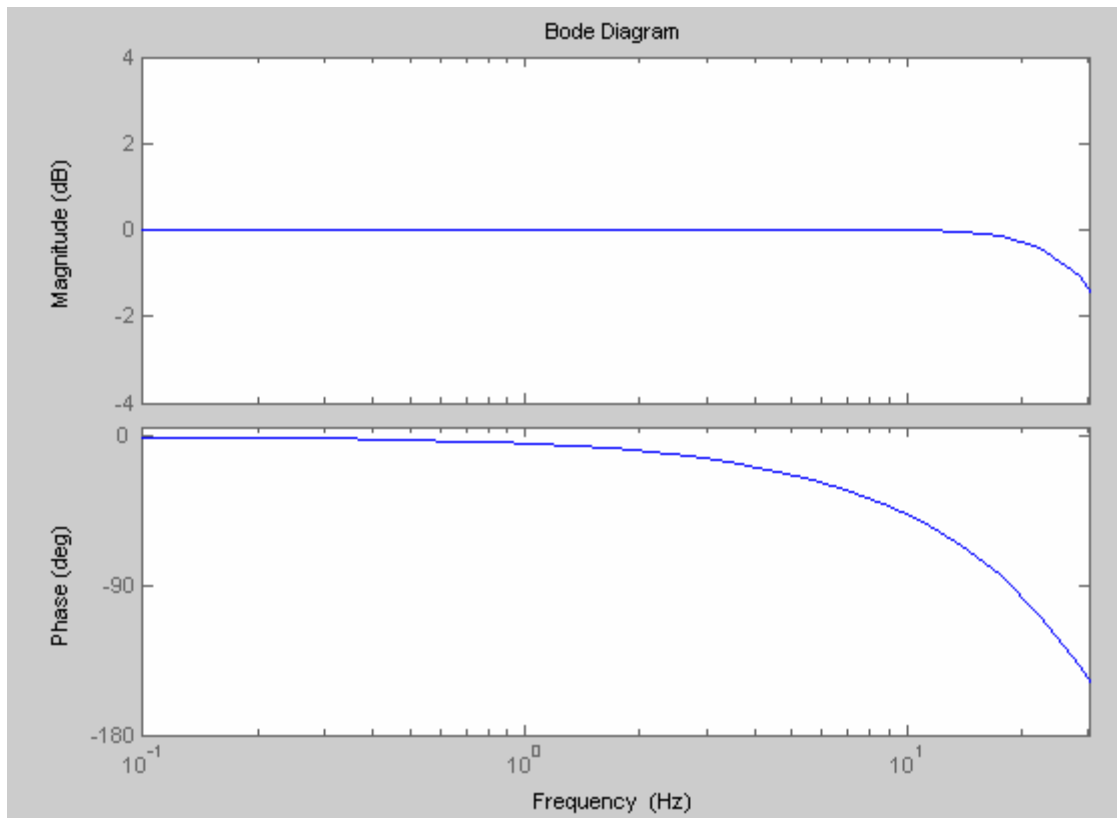


Figure 4.2: Transfer from reference to LVDT voltage of the closed loop system without time delay

The same closed loop transfer from reference to LVDT – voltage is measured for the dynamic system of the knee joint. Figure 4.3 shows this bodeplot.

The input for the measurement in figure 4.3 is a multi sine with frequencies from 0.1 to 30 Hz.. The gain and phase characteristics are an average of the frequencies of the multi sine. In the frequency range form 1 to 10 Hz, the system contains more noise than it does in the frequency range from 10 to 30 Hz. The coherence characteristic shows this behaviour too. The coherence of the frequency range from 1 to 10 Hz is between 0.8 and 0.9 and for the frequency range of 10 to 30 Hz between 0.9 and 1.

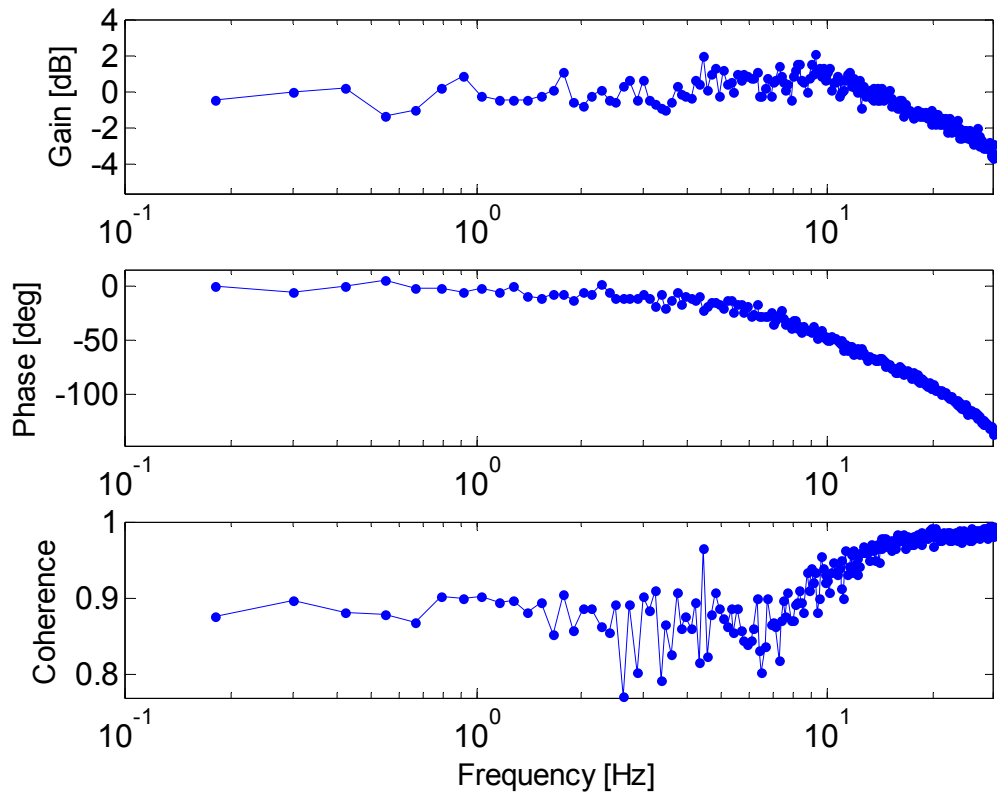


Figure 4.3: Bodeplot of the LQG controlled (closed loop) system, from reference to LVDT – voltage

The bodeplots of the figures 4.2 and 4.3 are comparable. The magnitude of the measurement decreases a little faster compared to that in the model. This difference can be caused by a summation of little parameter estimation errors, stick slip in the system or saturation symptoms of the motor. But the difference is small and the model is an acceptable estimation of the measurement. Both phase characteristics are almost the same. The phase lag of the model by 30 Hz is 146 degrees. The phase lag by 30 Hz for the measurement is 144 degrees.

The conclusion after comparing the bodeplots of the closed loop transfer of the model and the measurement is, that the model is a good estimation of the measurement. The models used for the controller are useful for model based control, like LQG.

The -3 dB point of the controlled system (measurement) for the measurement is about 30 Hz. This bandwidth of 30 Hz is enough for the operating range of this system. The -3 dB point of the model is not visible in the plot. The controller bandwidth is around the 38 Hz. The designed LQG controller controls the dynamic behaviour of the knee joint on an acceptable manner.

5. Conclusions and Recommendations

The first paragraph of this chapter describes the conclusions of modelling and controlling the dynamic system of the knee joint and an evaluation of the test results. The second paragraph contains a list of recommendations for further research and development.

5.1 Conclusions

The conclusions of the different topics presented in chapters 1 to 4 are given in this paragraph. First of all, a conclusion about the model, then a conclusion about the controller, and, finally, a conclusion about the test results.

Model

The Ideal Physical Model (IPM) described in chapter two contains all the important masses, inertias springs and dampers and is a good representation of the knee joint connected with the fixed world. The IPM is simplified. This mechanical model is a good starting point to get a block scheme of the dynamic system. After some tuning, the open loop transfer of the block scheme with the found parameters (also the motor friction) is comparable with the measurement. This 4th order model theoretically is a good representation of the real knee joint, but the huge differences of the values in the A matrix causes practical problems. The conversion of the 4th order model into a 2nd order model solves this problem. The 2nd order model is a good starting point for controller design.

Controller

The controller for the dynamic system of the knee joint is chosen in chapter three. The choice is the Linear Quadratic Gaussian controller based on state space technique. This control system consists of two parts, a Linear Quadratic Regular (LQR) and a Linear Quadratic Estimator (LQE). These two parts together give the optimal feedback gain. The matrices to get a controlled system which contains an acceptable error, together with realistic torque commands are:

$$\text{- for LQR} \rightarrow Q = \begin{bmatrix} 1 & 0 \\ 0 & 0 \end{bmatrix} \quad R = [10 * 10^{-3}]$$

$$\text{- for LQE} \rightarrow Q = [1] \quad R = [10 * 10^{-3}] \quad G = [1 ; 0.5]$$

The response of the controlled system with these settings has an absolute time delay of 0.01 s and satisfies the operating range of this system (around 4 Hz).

The controller can be kept stable for a coulomb friction increased with 380%, a viscous friction increased with 3420% and a friction rise of 220% for both frictions together.

Test results

The model is adapted after using a new measurement spring with different stiffness. A new controller is designed based on this adapted mode. The transfer function of the open loop system is measured and identified by Matlab (ident). The transfer function is:

$$H = \frac{5.867}{s^2 + 65.01 \cdot s + 4072} * e^{-s(0.007)}$$

The differences between the model and the identification are small. The identification is useful to find out the damping factor in the system. Both model and identification can be used for control design of the 2nd order model. The model is useful to give a prediction for the system behaviour without carrying out measurements.

The designed controller is tested on the knee joint. The closed loop transfer is determined and compared with the closed loop transfer of the simulation (model).

The static friction in the system can influence the performances of the system for small amplitudes. The closed loop system gives acceptable results for amplitudes above 1 millimetre.

The conclusion after comparing the bodeplots of the closed loop transfer of the model and the measurement is, that the model is a good estimation of the measurement. The models used for the controller are useful for model based control, like LQG.

The -3 dB points of the measurement and the -3 dB point of the simulation are near to each other. The bandwidth for the controlled knee joint is up to 30 Hz and the bandwidth for the simulation up to 38 Hz.

The designed LQG controller controls the dynamic behaviour of the knee joint in an acceptable manner.

The designed 4th order model is a good theoretical presentation of the dynamic system of the knee joint. The 4th order model gives huge differences in the values of the A matrix. These differences give numerical problems for control design. A 2nd order model solves these problems and the 2nd order model can be used for the design of the controller. The LQG controller gives satisfactory results during testing, both in simulation and in practice. The designed controller is robust and has enough bandwidth (-3 dB point around 30 Hz) for the operating frequency (5 Hz). The gentleness of the controlled system can not be determined at this moment, because the controller is designed for a situation in which the knee is connected with the fixed world.

5.2 Recommendations

To improve this control system for the knee joint, some further recommendations and future work are given for further research.

- **Expand** the model and controller (described in chapter 2 and 3) with a load at the shin element. This controller is designed with the knee in a fixed situation. The next step is to design a controller which is able to handle a knee with load.
- **Take** the second measurement point (motor decoder) into account by controlling the system. Find out the differences between control results with one and two measure points. Determine an optimal measurement with a combination of the two measure signals.
- **Design** of an identification algorithm to estimate the mass, stiffness, damping and delay of the system. The model can be adapted by these parameters. An optimal matched controller can be guaranteed by different parameters.
- **Carry out** a parameter variation research to find out to which extent the controller works acceptably.
- **MRAS** can be a good addition for this controller. It is an algorithm to find stability conditions using the method of Liapunov, for which the system is certainly stable [5]. A short explanation of this method is given in appendix B.

References

- [1] T Milner, Pathological gait, retrieved September 2004 from:
<http://www.sfu.ca/~tmilner/milner4.pdf>
- [2] R. Burie, Design and analyses of a force controlled Series Elastic Actuator (BW 156), Universiteit Twente, Enschede, December 2003
- [3] R. Kruidhof, Design of a gait rehabilitation robot (BW165), Universiteit Twente, Enschede, August 2004
- [4] prof.dr.ir J. van Amerongen, dr. Ir T.J.A de Vries, Digitale Regeltechniek, Universiteit Twente, Enschede, May 2002, blz 49
- [5] prof.dr.ir J. van Amerongen, Intelligent Control part 1 – MRAS, Universiteit Twente, Enschede, March 2004

A Data sheets

Technical data of the AC-synchronous motor SER3910

SER39x

Die 8-poligen AC-Synchronmotoren der Baureihe SER39x werden in den Varianten SER397, SER3910, SER3913 und SER3916 gebaut. Die Kantenlänge des Flanschs beträgt 85 mm. Aus der Tabelle können Sie die motorspezifischen Daten entnehmen:

Motorspezifische Daten

Motortyp			SER397	SER3910	SER3913	SER3916
Nennndaten						
Nennleistung	P_N	kW	0,35	0,69	1,0	0,84
Nenn Drehzahl ¹⁾	n_N	min^{-1}	6000	6000	6000	5000
Nenndauermoment	M_{dN}	Nm	0,55	1,1	1,6	1,6
Dauerstillstands- moment	M_{d0}	Nm	1,1	2,2	2,9	3,6
Maximale Werte						
Max. Spannung	U_{\max}	V_{AC}	480	480	480	480
		V_{DC}	680	680	680	680
max. Drehmoment	M_{\max}	Nm	4	8	11,5	14,5
max. zul. Drehzahl	n_{\max}	min^{-1}	6000	6000	6000	6000
max. Dauerleistung	$P_{d\max}$	kW	0,38	0,69	1,06	0,85
Drehmoment bei max. Dauerleistung	$M_{p_{d\max}}$	Nm	0,6	1,1	1,7	1,8
Drehzahl bei max. Dauerleistung	$n_{p_{d\max}}$	min^{-1}	6000	6000	6000	4500
Mechanische Werte						
Rotorträgheits- moment	J_R	kgcm^2	0,85	1,6	2,4	3,2
Gesamtlänge ²⁾	L	mm	141	171	201	231
Masse ²⁾	m	kg	2,2	3,3	4,4	6,1

1) für max. Leistung

2) ohne Bremse

Messwerte wurden ermittelt bei angeflanschten Motoren (Stahlplatte 300*300*10mm); Umgebungstemperatur 25°C; ohne Dichtring an der Antriebswelle

Gearbox: PLE 80, with ratio $i = 8$

size		PLE		PLE		PLE		PLE		Übersetzung/ratio $i^{(1)}$
		40	60	80	80/90	120	120/115	160		
moment of inertia ⁽²⁾	kgcm ²	0,031	0,135	0,77		2,63		12,14		3
		0,022	0,093	0,52		1,79		7,78		4
		0,019	0,078	0,45		1,53		6,07		5
		0,017	0,065	0,39		1,32		4,63		8
		0,030	0,131	0,74		2,62		–		9
		0,029	0,127	0,72		2,56		12,37		12
		0,023	0,077	0,71		2,53		12,35		15
		0,022	0,088	0,50		1,75		7,47		16
		0,019	0,075	0,44		1,50		6,65		20
		0,019	0,075	0,44		1,49		5,81		25
		0,017	0,064	0,39		1,30		6,36		32
		0,016	0,064	0,39		1,30		5,28		40
		0,016	0,064	0,39		1,30		4,50		64
		0,029	0,076	0,51		2,57		–		60
		0,019	0,075	0,50		1,50		–		80
		0,019	0,075	0,44		1,49		–		100
		0,029	0,064	0,70		2,50		–		120
		0,016	0,064	0,39		1,30		–		160
		0,016	0,064	0,39		1,30		–		200
		0,016	0,064	0,39		1,30		–		256
0,016	0,064	0,39		1,30		–		320		
0,016	0,064	0,39		1,30		–		512		
backlash	arcmin	< 30	< 20	< 12		< 8		< 6		1-stufig / 1-stage
		< 35	< 25	< 17		< 12		< 10		2-stufig / 2-stage
		< 40	< 30	< 22		< 16		–		3-stufig / 3-stage
torsional rigidity	Nm/arcmin	0,45	1,5	4,5		11		32,5		1-stufig / 1-stage
		0,47	1,5	5,2		11		35		2-stufig / 2-stage
		0,45	1,3	4,8		11		–		3-stufig / 3-stage
running noise ⁽³⁾	dB(A)	55	58	60		65		70		
⁴⁾ max. input speed ⁽²⁾	min ⁻¹	18000	13000	7000		6500		6500		
advised input speed ⁽⁴⁾	min ⁻¹	4500	4000	4000		3500		3000		

Springs

Materials:

Music wire: Din 17223 C/ No. 1.1200

Strain less steel wire: Din 17224/ X12CrNi 17.7 no. 1.4310

Tolerances: Din 2095-2/ Din 2098-2

Production:

Coiled Ends: Right hand

Ends: 0,2-0,8 mm squared and unground 1,0-10 mm squared and ground

Surface treatment:

The springs are oiled. Against an additional price, it is possible to supply them with other surface treatment. However, these are not on stock.

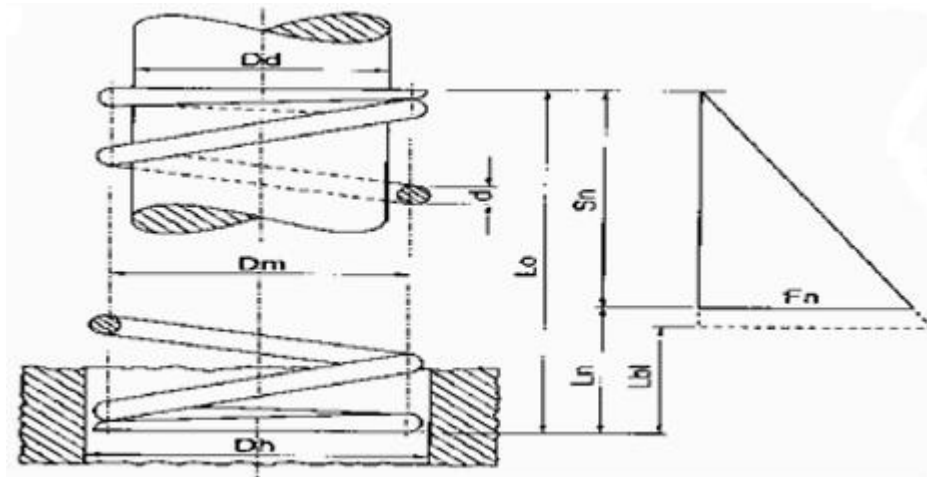
Formulas:

Spring rate: $C = F/s$

Shear modulus: $\pi = 8.F.Dm.k/\pi.d$

Load: $F = G . d^4 . s / 8 . Dm^3$.

Active coils: $nw = s.G.d^4 / 8.F.Dm^3$



Compression springs

Your input:

dm: 32

type of Material Music wire (Din norm = 17223-1.1200)

d	Dm	Nw	Lo	C N/mm	Sn	Fn	Number	Price category
4	32	5.5	79.5	14.42	46.2	666	D 13640	J
5	32	5.5	75	35.3	34.8	1226	D 13840	K
6.3	32	5.5	75	89.1	26	2315	D 14040	FA

B. Model Reference Adaptive Control (MRAS)

Introduction [5]:

Two questions:

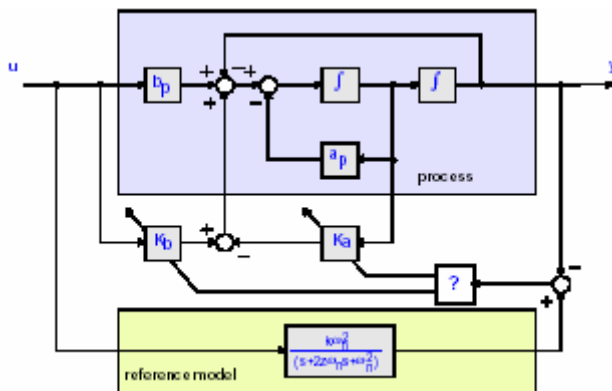
- 1) How to find a signal to control to control the true parameter just on time?
- 2) How to guarantee stability of an adaptive system, while adaptive systems are non-linear?

Two adaptive control systems:

- 1) systems with direct adjustment of the controller parameters, without explicit identification of the parameters of the process (direct adaptive control)
- 2) systems with indirect adjustment of the controller parameters, with explicit identification of the parameters of the process (indirect adaptive control)

Basic idea: the desired performance of the system is given by a mathematical model, the reference model. When the behaviour of the process differs from 'ideal' behaviour, which is determined by the reference model, the process is modified, either by adjusting the parameters of a controller or by generating an additional input signal for the process. This can be translated into an optimization problem, i.e minimization of the criterion:

$$C = \int_0^T e^2 dt \rightarrow e = y_m - y_p = x_m - x_p$$



Process and reference model

MIT rule:

$$K_b(t) = K_b(0) + \beta \int (eu) dt$$

$$K_a(t) = K_a(0) + \alpha \int (ex_2) dt$$

Stability approach:

5 steps to design a adaptive controller based on the Liapunov method

- 1) Determine the error differential equation:
$$\dot{e} = A_m \cdot e + Ax_p + bu$$
$$e = x_m - x_p$$
$$A = A_m - A_p$$
$$b = b_m - b_p$$
- 2) Choose a Liapunov function: $V(e) = e^T P e + a^T \alpha a + b^T \beta b$
- 3) Determine the conditions under which V (e) is definite negative
- 4) Solve P from $A_m^T P + P A_m = -Q$

Idea with regards to LOPES:

Due to the applied torque of the motor to the system, the system will be move. There will be a difference in model output and system output due to the opposite force, causes by friction and patient.

The state differences and output differences lead to an error differential equation. On the basis of Liapunov, the different states in the B matrix will adapted, such that a there will be a input gain.

The next adaptive laws can be determined:

$$K_a = \frac{1}{\alpha_{22}} \int_0^t (p_{21} \cdot e_1 + p_{22} \cdot e_2) x_n dt + K_a(0)$$

$$K_b = \frac{1}{\beta} \int_0^t (p_{21} \cdot e_1 + p_{22} \cdot e_2) u dt + K_b(0)$$